ACS OMEGA

http://pubs.acs.org/journal/acsodf

Review

The Resistance of SO_2 and H_2O of Mn-Based Catalysts for NO_x Selective Catalytic Reduction with Ammonia: Recent Advances and Perspectives

Jungang Tang, Xuetao Wang,* Haojie Li, Lili Xing, and Mengjie Liu

Cite This: *ACS Omega* 2023, 8, 7262−7278

Read Online

ACCESS | Metrics & More | Article Recommendations

ABSTRACT: The treatment of NO_x has become an urgent issue due to it being difficult to degrade in air and its tremendous adverse impact on public health. Among numerous NO_x emission control technologies, the technology of selective catalytic reduction (SCR) using ammonia (NH_3) as the reducing agent (NH_3-SCR) is regarded as the most effective and promising technique. However, the development and application of high-efficiency catalysts is severely limited due to the poisoning and deactivation effect by SO_2 and H_2O vapor in the low-temperature NH_3-SCR technology. In this review, recent advances in the catalytic effects from increasing the rate of the activity in low-temperature NH_3-SCR by manganese-based catalysts and the stability of resistance to H_2O and SO_2 during catalytic denitration are reviewed. In addition, the denitration reaction mechanism, metal modification, preparation methods, and structures of the catalyst are highlighted, and the challenges and potential solutions for the design of a catalytic system for degenerating NO_x over Mn-based catalysts with high resistance of SO_2 and H_2O are discussed in detail.

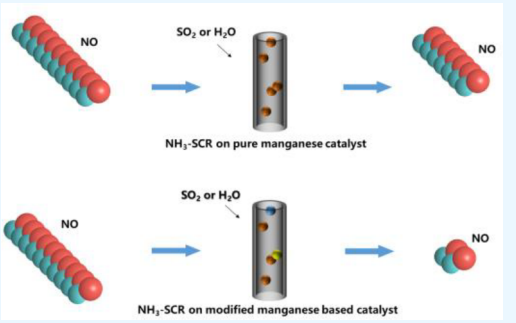

1. INTRODUCTION

Among the denitrification technologies of flue gas, high selectivity, high denitration conversion, and low NH_3 leakage rate were contained by the selective catalytic reduction (SCR), and the core of the SCR was catalysts.[1−3] V_2O_5+WO_3(MoO_3)/TiO_2 was the most popular commercial SCR catalyst due to its excellent catalytic performance and strong stability. However, due to the limitation of the narrow temperature window (300−400 °C), the vanadium titanium catalyst must be arranged in front of the desulfurization and dedusting devices.[4−9] This arrangement exposes the catalyst to an environment of high temperature, high dust, and high SO_2. Long-term operation is likely to lead to catalyst blockage and SO_2 poisoning and deactivation, and the active component V has strong biological toxicity, which may cause secondary pollution. The toxicity of vanadium also causes difficulties for the disposal of the waste catalysts, which hinders further applications of V-based oxide catalysts.[10,11] For this reason, a plethora of efforts have been made on developing low-temperature catalysts. The transition metals and their oxides have demonstrated considerable potential in replacing V-based catalysts. As a transition metal element, Mn has rich variable valence states, high electron mobility, and high redox performance at low temperature.[12−15] However, the stability of Mn-based catalysts is poor, which limits practical application of the catalyst especially the resistance to SO_2 and H_2O. Focus has centered on the research progress on water and sulfur resistance of Mn-based catalysts. Be that as it may, Mn-based catalysts are easily deactivated by SO_2 at low temperature, since SO_2 can be oxidized in the presence of Mn to form metal sulfate and ammonium sulfate species. Hence, an urgent need exists for the preparation of Mn-based catalysts that have significant SCR activity, sulfur and water resistance characteristics, and wide working temperature windows.

Nowadays, optimizing the performance of Mn-based catalysts with doped active metal is a research hotspot. Zhang et al.[16] prepared a series of MnM/palygorskite (PG) (M = La, W, Mo, Sb, Mg) for low-temperature NH_3-SCR denitration. The $MnSb_{0.156}$/PG possessed high NO_x conversion in the presence of SO_2 at low temperature, indicating that the SO_2 tolerance of the catalyst was effectively improved with addition of Sb. Shi et al.[17] prepared a series of Ce-modified La−Mn catalysts. Ce−La−Mn catalysts possessed 95% NO_x conversion in the presence of SO_2 and H_2O at 200 °C. In addition to doping active metals, scholars have studied other ways to improve the catalyst resistance, including renewing the support, manufacturing special structures, and

Received: October 26, 2022
Accepted: January 11, 2023
Published: February 16, 2023

https://doi.org/10.1021/acsomega.2c06796
ACS Omega 2023, 8, 7262−7278

selecting suitable preparation methods. Raja et al.[18] improved the denitrification stability of Mn/TiO_2, and $Mn-Cu_5/Ti$-CNT had excellent SO_2 and H_2O resistance. One of the reasons was that the doping of Cu promoted the production of Mn^{4+}. In addition, the addition of carbon nanotubes increased the specific surface area and total pore volume and reduced the average pore size of the catalyst. Wang et al.[19] prepared a series of 3DOM (three-dimensionally ordered macroporous)-$Mn_xCe_yTi_z$ catalysts. Both the 3DOM-Mn_3Ce_1 and 3DOM-$Mn_3Ce_1Ti_1$ catalysts had excellent water resistance. Chen et al.[20] prepared $Ce-Mn/TiO_2$ catalysts using reverse coprecipitation, conventional coprecipitation, and impregnation methods. The $Ce-Mn/TiO_2$ catalysts prepared by the reverse precipitation method had the best SO_2 resistance. The possible reason is that the catalysts prepared by this method have high dispersion, large specific surface area, excellent redox properties, and numerous acid sites. In this paper, these methods will be introduced in detail. Moreover, the advantages and limitations over different catalysts are pointed out and future development direction is proposed. The Mn based SCR catalysts with excellent resistance to SO_2 and H_2O is summarized in Table 1. The table is introduced in the order of no-load, load, and special structure. Each part is introduced according to the number of active metal doping from simple to complex. The information in the table and the content in the text complement each other.

2. THE MECHANISM OF SCR AND DEACTIVATION MECHANISM ABOUT SO_2 AND H_2O

2.1. The Mechanism of SCR. In ammonia selective catalytic reduction technology, the main reaction of low-temperature SCR reaction refers to the reaction in which NH_3 reduces NO to N_2 and generates H_2O. Moreover, two reaction pathways are constituted with the differences in intermediate reactions, namely, L-H mechanism and E-R mechanism. The L-H mechanism is a double adsorption mechanism. NH_3 and NO are adsorbed on the catalyst surface, as shown in eqs 1 and 2. The adsorbed NO is oxidized to nitrous acid by Me^{n+}, as shown in eq 3. In addition, adsorbed ammonia reacts with these species to form ammonium nitrite, which is then decomposed into nitrogen, as shown in eq 4. The E-R mechanism is a single adsorption mechanism. The adsorbed ammonia reacts with gaseous NO, and the detailed process is shown in formulas 5−8.

The L-H mechanism is shown below:

$$NH_{3(g)} \rightarrow NH_{3(ad)} \quad (1)$$

$$NO_{(g)} \rightarrow NO_{(ad)} \quad (2)$$

$$Me^{n+} = O + NO_{(ad)} \rightarrow Me^{(n-1)+}-O-NO \quad (3)$$

$$NH_{3(ad)} + Me^{(n-1)+}-O-NO \rightarrow Me^{(n-1)+}-O-NO-NH_3 \rightarrow Me^{(n-1)+}-OH + N_2 + H_2O \quad (4)$$

Me represents active center of metal atom in the reaction equation.

The E-R mechanism is shown below:

$$NH_{3(g)} \rightarrow NH_{3(ad)} \quad (5)$$

$$NH_{3(ad)} + Me^{n+} = O \rightarrow [NH_2]_{(ad)} + Me^{(n-1)+}-OH \quad (6)$$

$$[NH_2]_{(ad)} + NO_{(g)} \rightarrow NH_2NO \rightarrow N_2 + H_2O \quad (7)$$

$$Me^{(n-1)+}-OH + 1/4O_2 \rightarrow Me^{n+} = O + 1/2H_2O \quad (8)$$

2.2. The Deactivation Mechanism of SO_2 and H_2O. Nowadays, high sulfur content is contained in the coal used in China. In low-temperature NH_3-SCR system, a denitrification device is usually placed behind the desulfurization device. However, a small amount of SO_2 could cause the low-temperature denitration performance of the catalyst to be reduced or even deactivated.[50] Therefore, a catalyst with high sulfur resistance and achieving commercial application for environmental treatment needs to be developed in China. The SO_2 inactivation mechanism of four types may be contained. First, denitration efficiency is reduced with the ammonium sulfate generated by the reaction between SO_2 and NH_3. Second, SO_2 forms a competitive adsorption with NO. Third, metal sulfate is formed. Fourth, gaseous SO_2 is easily oxidized to SO_3 on the catalyst surface, which forms polysulfuric acid. Kwon et al.[51] explored the resistance to SO_2 of the NH_3-SCR catalyst and found that SO_2 and NH_3 generated $(NH_4)_2SO_4$ and NH_4HSO_4 on the V/Sb/Ti catalysts. Additionally, ammonium salts were difficult to decompose at low temperature and blocked the SCR reaction active sites. Sheng et al.[52] studied the low-temperature NH_3-SCR resistance of $Mn-Ce/TiO_2$ catalyst to SO_2 and found that the Mn/TiO_2 catalyst could be sulfated by SO_2 to form stable $Mn(SO_4)_x$, which led to the deactivation of the catalyst. Zhang et al.[53] proposed that SO_2 was easily oxidized to SO_3 on the MnO_x/palygorskite (PG) catalyst surface, resulting in the formation of polysulfuric acid, the encapsulation of active components, and the blockage of micropores. Jiang et al.[54] studied the influence of SO_2 on Fe-Mn/TiO_2 low-temperature SCR catalyst, which showed that the adsorption capacity of SO_2 surpassed that of NO, thus occupying the adsorption site of NO. Yu et al.[55] investigated the deactivation mechanism of $MnO_2-Fe_2O_3-CeO_2-TiO_2$ catalyst in the presence of SO_2. The results demonstrated that SO_2 did not form $MnSO_4$ directly with MnO_x. $MnSO_4$ was formed by the combination of SO_3 with MnO. SO_3 in this reaction was derived from the decomposition of $(NH_4)_2SO_4$. The SO_2 deactivation mechanisms may have cross-linkages, and the toxicants also may have a certain connection, from which the degree of catalyst poisoning was likely to be strengthened. Each deactivation mechanism refused to intersect, so the resistance to SO_2 was likely to be improved. Thus, the mechanism of SO_2 deactivation may require further research.

The remarkable deactivation of the catalyst results from the high content of the water vapor in flue gas. There were two types of inactivation mechanisms of H_2O. First, H_2O competed with NH_3 and NO for adsorption, occupying the active sites on the catalyst surface and blocking the catalyst pores. Second, SO_2 poisoning was aggravated by H_2O. Xiong et al.[56] comparatively studied the adsorption performance of Mn−Fe spinel catalysts for NH_3 and NO_x in the presence or absence of H_2O. The results showed that the adsorption performance of the catalysts for NH_3 and NO_x decreased in the presence of H_2O. Phil et al.[57] investigated the resistance to SO_2 of low-temperature V_2O_5/TiO_2 catalysts for NH_3-SCR and found that the number of Bronsted sizes was increased with the increase

https://doi.org/10.1021/acsomega.2c06796
ACS Omega 2023, 8, 7262−7278

Table 1. Summary of the Current Status of the Resistance to SO_2 and H_2O on Mn-Based Catalysts in the Literature[a]

catalyst	reaction conditions	T (°C)	X_{NO}	t (h)	X_{NO}-U-SO_2	X_{NO}-A-SO_2	X_{NO}-U-H_2O	X_{NO}-A-H_2O	X_{NO}-U-SO_2+H_2O	X_{NO}-A-SO_2+H_2O	ref
Fe-MnO_x	1000 ppm of NH_3, 1000 ppm of NO, 3% O_2, 5% H_2O, 100 ppm of SO_2, 5% H_2O+100 ppm of SO_2GHSV at 30,000 h^{-1}	120	99%	4, 4, 4	90%	97%	87%	94%	91%	92%	21
Cr-MnO_x	1000 ppm of NH_3, 1000 ppm of NO, 3% O_2, 100 ppm of SO_2GHSV at 30,000 h^{-1}	120	98%	3, /, /	83%	96%					22
CoMnO_x	500 ppm of NH_3, 500 ppm of NO, 5% O_2, 5% H_2O, 50 ppm of SO_2GHSV at 80,000 h^{-1}	180	100%	10, 8, /	62%		95%	100%			23
MnEuO_x	600 ppm of NH_3, 600 ppm of NO, 5% O_2, 5% H_2O+100 ppm of SO_2, GHSV at 108,000 h^{-1}	350	100%	/, /, 2					89%	94%	24
Ce-FeMnO_x	1000 ppm of NH_3, 1000 ppm of NO, 3% O_2, 5% H_2O, 100 ppm of SO_2, 10% H_2O+100 ppm of SO_2GHSV at 30,000 h^{-1}	120	99%	4, 4, 4	96%	99%	92%	99%	76%	97%	25
Ni-Mn-Ti	1000 ppm of NH_3, 1000 ppm of NO, 3% O_2, 15% H_2O, 100 ppm of SO_2, 15% H_2O+100 ppm of SO_2GHSV at 40,000 h^{-1}	240	99%	10, 15, 15	99%		95%		94%		26
FeMnZr	500 ppm of NH_3, 500 ppm of NO, 4% O_2, 100 ppm of SO_2GHSV at 35,000 h^{-1}	200	99%	25, /, /	97%						27
Mn-Eu-Fe	500 ppm of NH_3, 500 ppm of NO, 5% O_2, 15% H_2O, 50 ppm of SO_2, 15% H_2O+50 ppm of SO_2GHSV at 75,000 h^{-1}	230	97%	5, 50, 30	92%		88%	96%	63%		28
Co−Mn−CeO_x	500 ppm of NH_3, 500 ppm of NO, 5% O_2, 10% H_2O, 150 ppm of SO_2, 5% H_2O+100 ppm of SO_2GHSV at 48,000 h^{-1}	175	91%	4, 6, 6	78%	88%	80%	91%	77%	91%	29
SmMnNiTiO_x	1000 ppm of NH_3, 1000 ppm of NO, 3% O_2, 5% H_2O, 100 ppm of SO_2, 5% H_2O+100 ppm of SO_2GHSV at 40,000 h^{-1}	240	100%	7, 7, 7	96%	100%	90%	100%	84%	100%	30
MnSmZrTiO_x	500 ppm of NH_3, 500 ppm of NO, 5% O_2, 2.5% H_2O, 100 ppm of SO_2, 2.5% H_2O+100 ppm of SO_2GHSV at 30,000 h^{-1}	200	100%	24, 12, 19	87%	97%	96%		83%	96%	31
MnO_x/$ZrTiO_2$	500 ppm of NH_3, 500 ppm of NO, 4% O_2, 5% or 10% H_2O, 200 ppm of SO_2GHSV at 35,000 h^{-1}	200	100%	30, 30, /	70%	70%	100%	100%			32
Mn/TiO_2	500 ppm of NH_3, 500 ppm of NO, 5% O_2, 10% H_2O, 100 ppm of SO_2, 10% H_2O+100 ppm of SO_2GHSV at 40,000 h^{-1}	150	100%	4, 4, 4	82%	96%	82%	93%	68%	89%	33
Mn-MOF-74	1000 ppm of NH_3, 1000 ppm of NO, 2% O_2, 100 ppm of SO_2, 5% H_2O+100 ppm of SO_2GHSV at 40,000 h^{-1}	220	97%	3, /, 3	88%	95%			85%	95%	34
MnEu/TiO_2	600 ppm of NH_3, 600 ppm of NO, 5% O_2, 100 ppm of SO_2	150	85%	25, /, /	70%	75%					35
Mn-Ce/TiO_2	1000 ppm of NH_3, 1000 ppm of NO, 3% O_2, 100 ppm of SO_2GHSV at 40,000 h^{-1}	150	100%	6.5, /, /	84%						36
Mn-Sm/TiO_2	500 ppm of NH_3, 500 ppm of NO, 5% O_2, 5% H_2O, 100 ppm of SO_2, 5% H_2O+100 ppm of SO_2GHSV at 80,000 h^{-1}	200	91%	2, 2, /	80%	89%	91%	91%			37
Cu-Mn/TiO_2	800 ppm of NH_3, 720 ppm of NO, 3% O_2, 100 ppm of SO_2GHSV at 30,000 h^{-1}	180	98%	10, /, /	84%	84%					38
Fe-Mn/TiO_2	1000 ppm of NH_3, 1000 ppm of NO, 2% O_2, 2.5% H_2O, 2.5% H_2O+100 ppm of SO_2GHSV at 30,000 h^{-1}	150	100%	/, 5, 5			90%	100%	90%	100%	39
FeMnCe/γ-Al_2O_3	700 ppm of NH_3, 700 ppm of NO, 3% O_2, 10% H_2O, 350 ppm of SO_2, 10% H_2O+350 ppm of SO_2GHSV at 10,000 h^{-1}	250	96%	3, 3, 4	90%	96%	88%	96%	79%	96%	40
Fe-Mn-Ce/TiO_2	600 ppm of NH_3, 600 ppm of NO, 3% O_2, 3% H_2O+100 ppm of SO_2GHSV at 50,000 h^{-1}	180	95%	/, /, 6					83%	86%	41
Mn-Ce-Pd/GR	500 ppm of NH_3, 500 ppm of NO, 5% O_2, 200 ppm of SO_2GHSV at 24,000 h^{-1}	160	100%	4, /, /	66%	95%					42
Fe-Ce-Mn/ACF_N	500 ppm of NH_3, 500 ppm of NO, 5% O_2, 10% H_2OGHSV at 20,000 h^{-1}		91%	/, 5.5, /			76%	91%			43
Mn-Ce-V/AC	500 ppm of NH_3, 500 ppm of NO, 5% O_2, 100 ppm of SO_2, 10% H_2O+100 ppm of SO_2GHSV at 18,000 h^{-1}	200	99%	8, /, 8	88%	88%			81%	81%	44
nf-MnO_x@CNTs	500 ppm of NH_3, 500 ppm of NO, 3% O_2, 4% H_2OGHSV at 48,000 h^{-1}	225	100%	/, 5, /			100%	100%			45
CeO_2-MnO_2	800 ppm of NH_3, 800 ppm of NO, 5% O_2, 100 ppm of SO_2GHSV at 40,000 h^{-1}	220	100%	6, /, /	75%	78%					46
Fe@Mn@CNTs	550 ppm of NH_3, 550 ppm of NO, 5% O_2, 100 ppm of SO_2, 10% H_2O+100 ppm of SO_2GHSV at 20,000 h^{-1}	240	97%	4, /, 4	94%	95%			91%	97%	47
meso-TiO_2@MnCe/CNTs	500 ppm of NH_3, 500 ppm of NO, 3% O_2, 200 ppm of SO_2GHSV at 10,000 h^{-1}	300	98%	4.5, /, /	95%	98%					48

https://doi.org/10.1021/acsomega.2c06796
ACS Omega 2023, 8, 7262−7278

Table 1. continued

catalyst	reaction conditions	T (°C)	X_{NO}	t (h)	X_{NO}-U-SO_2	X_{NO}-A-SO_2	X_{NO}-U-H_2O	X_{NO}-A-H_2O	X_{NO}-U-SO_2+H_2O	X_{NO}-A-SO_2+H_2O	ref
Mn/CeO_2-MSs	500 ppm of NH_3, 500 ppm of NO, 5% O_2, 5% H_2O, 50 ppm of SO_2GHSV at 36,000 h^{-1}	210	100%	4, 6, /	97%		85%	100%			49

[a] t (h), X_{NO}, X_{NO}-U, and X_{NO}-A represent the time of the resistance tests on different poisons (SO_2, H_2O, and SO_2+H_2O), the NO_x conversion of conventional SCR reaction, the NO_x conversion under resistance test and after resistance test, respectively.

of water vapor concentration at low temperature. NH_3 combined with the Bronsted sites formed NH_4^+, while SO_2 and SO_3 combined with the NH_4^+ to form ammonium salts, which enhanced the toxic effect of SO_2. In general, the effect of H_2O on the catalyst is generally reversible, while the inhibitory effect of SO_2 on the catalyst is remarkable and irreversible, as shown in Figure 1.

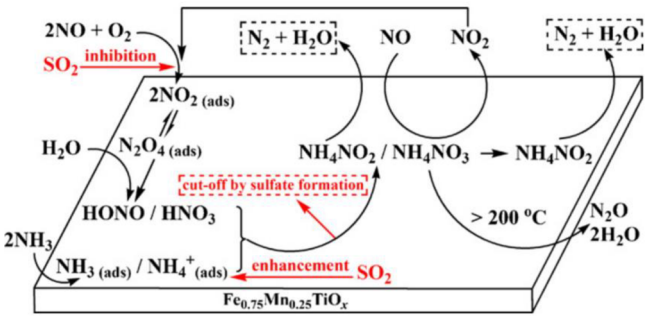

Figure 1. Mechanism of the NH_3-SCR reaction and the influence of SO_2 and H_2O on the reaction pathway. Reprinted with permission from 58. Copyright 2010 Elsevier.

3. THE OPTIMIZATION OF Mn-BASED CATALYST

The Mn-based catalyst has multiple valence states such as Mn^{2+}, Mn^{3+}, and Mn^{4+}, due to the orbital arrangement of Mn element $3d_54s_2$, which ensures high redox performance of Mn-based catalyst and the high activity of single MnO_x catalyst at low temperature. However, the SO_2 and H_2O tolerance of the catalyst is poor. In order to improve the sulfur resistance of the catalyst, four strategies have been presented by researchers. First, during the process of sulfate formation, the adsorption and oxidation of SO_2 on the catalyst surface play an important role. Second, changing or enhancing the active interlocutor species makes the effect of SO_2 on the SCR reaction weaker. Third, the main active sites are protected with the construction of sacrificial sites. Fourth, the purpose of improving the sulfur resistance of the catalyst can also be achieved by promoting the decomposition of sulfate species. As shown in Figure 2, metal

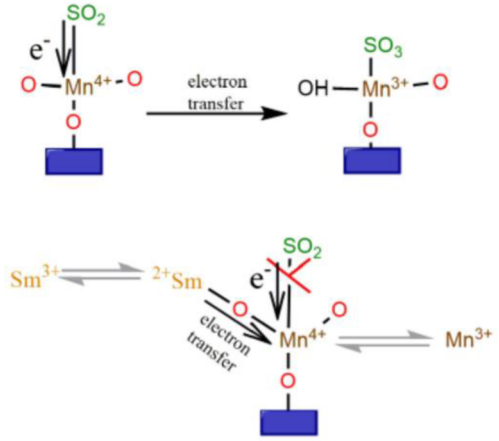

Figure 2. Diagram for the suppressed oxidation of SO_2 to SO_3. Reprinted with permission from ref 31. Copyright 2018 Elsevier.

sulfates are formed with electron transfer between SO_2 and Mn^{4+}. The addition of Sm results in the transfer of electrons

https://doi.org/10.1021/acsomega.2c06796
ACS Omega 2023, 8, 7262−7278

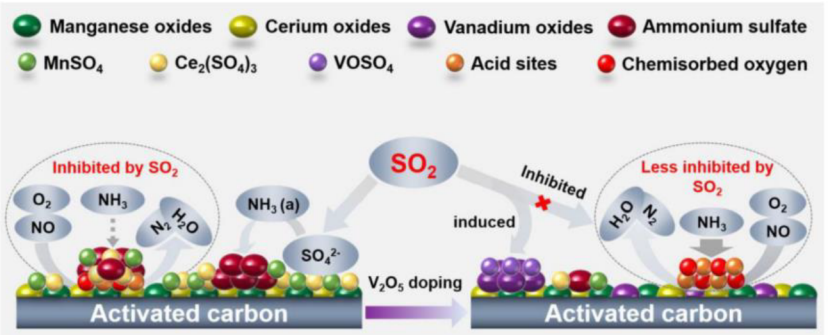

Figure 3. Scheme of V as trapper. Reprinted with permission from ref 44. Copyright 2019 Elsevier.

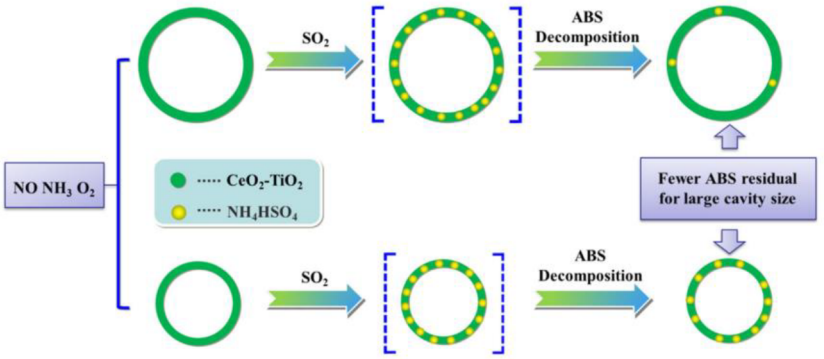

Figure 4. Effect of cavity size for ABS decomposition. Reprinted with permission from ref 59. Copyright 2019 Elsevier.

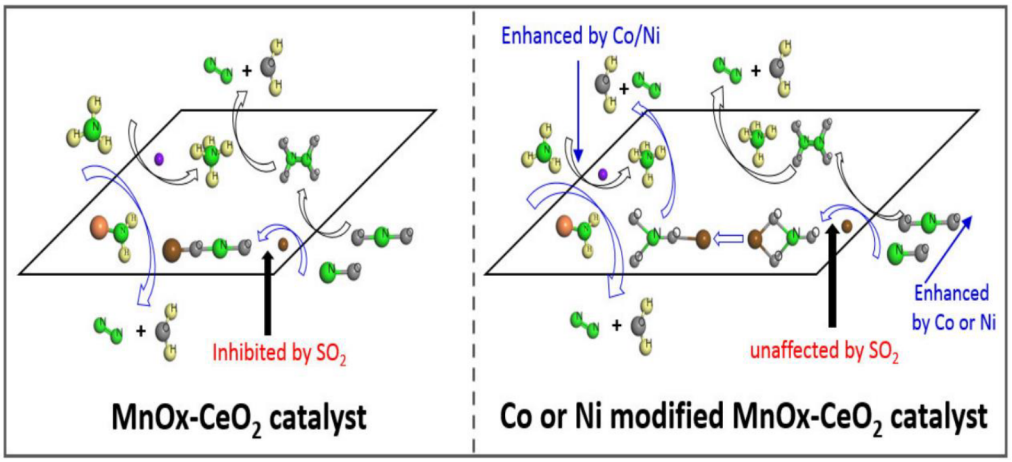

Figure 5. Influences of SO_2 on SCR mechanism over $Mn_4Ce_6O_x$, $Ni_1Mn_4Ce_5O_x$, and $Co_1Mn_4Ce_5O_x$ catalysts. Reprinted with permission from ref 29. Copyright 2017 Elsevier.

from Sm^{2+} to Mn^{4+} instead of SO_2, which prevents the oxidation of SO_2 and eventually reduced the metal sulfate. As displayed in Figure 3, SO_2 forms SO_4^{2-} on the catalyst surface and combines with NH_3 to form ammonium salts. After V_2O_5 modification, V_2O_5 traps SO_2 and prevents the formation of ammonium salt. As shown in Figure 4, In a large cavity, the rate of the decomposition on ammonium salts is more rapid. As shown in Figure 5, The monodentate nitrite species on the surface of MnO_x-CeO_2 are inhibited by SO_2. The NO_x species adsorbed on the surface of catalyst Co(Ni)-MnO_x-CeO_2 is generally a bidentate nitrate without influences by SO_2. The catalyst can still react along the L-H mechanism. In addition, researchers have made some progress in the H_2O tolerance of catalysts. As shown in Figure 6, The NO desorption amount of

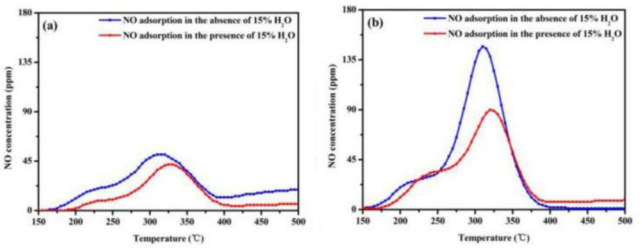

Figure 6. TPD of NO on (a) Mn-Eu-550 and (b) Mn-Eu-Fe-500 catalysts. Reprinted with permission from ref 28. Copyright 2019 Wiley.

https://doi.org/10.1021/acsomega.2c06796
ACS Omega 2023, 8, 7262−7278

Mn-Eu-Fe-500 is higher than that of Mn-Eu-550 before and after the modification, which may be an essential reason for the excellent H_2O resistance of Mn-Eu-Fe-500. Within a short time, the SO_2 poisoning can effectively be weakened with the reduction of SO_2 adsorption and oxidation, the construction of the sacrificial sites to the protecting active site, and promoting the decomposition rate of the sulfate species. Combining these strategies, the consumption of the constructed sacrificial sites may be decreased with reduced adsorption and oxidation of SO_2 and increased decomposition rate of the sulfate species. Accordingly, an effective long-term application catalyst may be obtained. Metal doping type, supported type, special structure type, and optimized preparation method type are contained in specific methods.

3.1. Metal Doping. A Mn-based catalyst has high denitration activity. However, the stability of the catalyst is poor. Denitration performance and stability can be improved with the catalyst-doped active metals. From the view of physicochemical properties, the morphology and structure of the material can be changed, the dispersion of active sites can be increased, grain size can be reduced, and redox performance and surface acidity can be improved by doping active metals. From the catalytic point of view, catalytic activity, selectivity, and the poison resistance can be improved by doping active metals. Suitable calcination temperature, high redox performance, excellent acidity, and low surface area loss are beneficial to improve the SO_2 and H_2O resistance of the catalyst.[25,28] The resistance of the catalyst to SO_2 and H_2O could be improved by doping MnO_x with other oxides.[5] The Mn-based SCR catalyst with doped active metals has been extensively studied. As shown in Figure 7, in the presence of SO_2, the

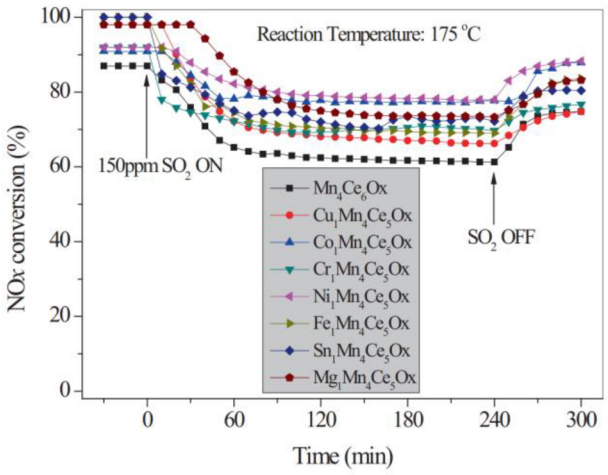

Figure 7. Resistance to SO_2 over $MnCeO_x$, $CuMnCeO_x$, $CoMnCeO_x$, $CrMnCeO_x$, $NiMnCeO_x$, $FeMnCeO_x$, $SnMnCeO_x$, and $MgMnCeO_x$ at 175 °C. Reaction conditions: [NO] = [NH_3] = 500 ppm, [O_2] = 5 vol %, [SO_2] = 150 ppm, [H_2O] = 10 vol %, N_2 to balance, total flow rate = 200 mL/min, GHSV = 48000 h^{-1}. Reprinted with permission from ref 29. Copyright 2017 Elsevier.

resistance of the catalyst to SO_2 can be improved with various doped active metals on the basis of Mn−Ce catalyst. After stabilization, the order of the NO_x conversion from high to low is Ni, Co, Mg, Sn, Cr, Fe, and Cu. CeO_2 is frequently used as a MnO_x dopant. France et al.[25] optimized $FeMnO_x$ and found the decomposition of ammonium salts might be accelerated by doped Ce. Besides, the loss of the intermediate active species can be reduced, and the main active metal components can be protected by doped Ce. A fast SCR reaction could not only improve NO_x removal efficiency but also inhibit SO_2 adsorption.[60] The formation of oxygen vacancies on the surface of the catalyst was promoted with the redox cycle between Ce^{4+} and Ce^{3+}, which could effectively promote the oxidation of NO to NO_2 at low temperature,[61,62] thus increasing the fast SCR reaction. A high denitrification performance Mn−Ce catalyst was obtained by Chen et al.[63] The NO_x conversion was increased from 92.6 to 97.8% at 150 °C with 200 ppm of SO_2. Superior SO_2 resistance might be attributed to the porous structure formed by the Mn−Ce oxide. In addition to Ce, Fe was also considered as an ideal additive to improve the denitration performance of Mn-based SCR catalysts.[64] Doped Fe is beneficial for improving the resistance to SO_2 and H_2O. After doping Fe, NO oxidation is greatly enhanced with the presence of a high redox potential pair of Fe and Mn.[21] Guo et al.[28] found the Mn−Eu−Fe catalyst doped with Fe had a high surface Fe^{3+} concentration, a low binding energy of Fe^{3+} and Fe^{2+}, a high O_α quantity, a high redox performance, and more acid content, which were beneficial for improving the resistance to H_2O. Besides, Mn−Eu−Fe had the best H_2O resistance when then calcination temperature was 500 °C. Doping of Sm has been widely used and studied because the redox ability, specific surface area, and sulfur resistance of the catalyst can be greatly improved. Pure SmO_x has almost no effect on the low-temperature NH_3-SCR reaction. However, the resistance to H_2O and SO_2 is significantly improved when Sm is doped into Sm−Mn mixed oxide catalysts.[65] The $Sm_aMnNi_2Ti_7O_x$ catalysts (a = 0.1, 0.2, 0.3, 0.4) were prepared by Tong et al.[30] The oxidation of SO_2 to SO_3 can be restrained by the doped Sm. This is possibly due to the suppressed electron transfer from SO_2 to Mn^{4+}. Qin et al.[66] compared the SO_2 resistance of $MnTiSnO_x$ and $SmMnTiSnO_x$ catalysts and obtained similar results. In addition to Ce, Fe, and Sm doping, doping with other elements has also been studied. Chen et al.[22] prepared Mn−Cr mixed oxides by the citric acid method and found that $CrMn_{1.5}O_4$ was formed with the introduction of Cr, which significantly improved the SO_2 tolerance of the catalyst. The Mn catalyst doped with Co exhibited excellent water resistance due to a relatively large specific surface area and orderly pore structure inside the catalyst.[36,67] Additionally, the Co-doped catalyst has a remarkable resistance to SO_2. The $Co_1Mn_4Ce_5O_x$ and $Ni_1Mn_4Ce_5O_x$ catalysts prepared by Gao et al.[29] could maintain a NO_x conversion of 78% at 175 °C in an atmosphere of 150 ppm of SO_2. The main reactants of the $Co_1Mn_4Ce_5O_x$ and $Ni_1Mn_4Ce_5O_x$ catalysts were not inhibited by SO_2. The Cu-modified Mn-based catalyst appears to not only have high activity but also maintain stable resistance to SO_2 and H_2O, which is a potential doped active metal. Wang et al.[68] prepared a series of AMn_2O_4 (A = Cu, Co) catalysts and found that catalytic activity of $CuMn_2O_4$ was higher than that of $CoMn_2O_4$, while the tolerance of $CuMn_2O_4$ was excellent at 100 ppm of SO_2 and 10 vol % H_2O. Chen et al.[26] prepared $Ni_xMn_{1-x}Ti_{10}$ catalysts. The oxidation of SO_2 to SO_3 was restrained with doped Ni. Chang et al.[69] found that the resistance to H_2O and SO_2 was significantly improved with doped Sn. The thermogravimetric analysis (TGA) showed that the main peaks of the Sn−Mn−Ce−O catalysts shifted to lower temperature. Guo et al.[27] found that the interaction of Fe, Mn, and Zr on the $Fe_{0.3}Mn_{0.5}Zr_{0.2}$ catalyst protected the active ingredients from vulcanization. The catalyst-doped Eu

https://doi.org/10.1021/acsomega.2c06796
ACS Omega 2023, 8, 7262−7278

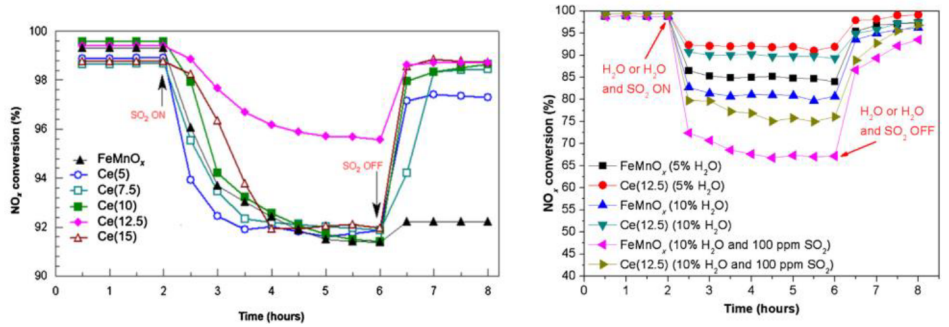

Figure 8. Influence of SO_2 and H_2O or combined H_2O and SO_2 on NO_x conversion of $FeMnO_x$ and $FeMnCeO_x$. Reaction conditions: [NO] = [NH_3] = 0.1%, [H_2O] = 5 or 10%, [SO_2] = 100 ppm, [O_2] = 3%, N_2 to balance, GHSV = 30,000 h^{-1}; reaction temperature = 120 °C. Reprinted with permission from ref 25. Copyright 2017 Elsevier.

also had excellent resistance to H_2O and SO_2.[24] To sum up, the adsorption and oxidation of SO_2 can be inhibited by the Mn-based catalyst-doped Fe, Sm, and Ni, the active ingredients can be protected by the doped Zr, the sulfate decomposition can be accelerated by the doped Sn, and the intermediate adsorbed species can be protected by the doped Co. The Ce can accelerate the decomposition of sulfate, enhance the adsorption of intermediate species, and build sacrifice points. Besides, the adsorption and oxidation of SO_2 can be reduced by the doped Ce. This comprehensive influence appears to be the reason why the SO_2 resistance can be greatly improved by Ce as an additive. Additionally, the Ce and Fe are often used as the first doped active metals of Mn-based catalysts. The composite Mn-based catalysts with more excellent sulfur resistance can often be obtained by doping appropriate second active metals. However, only the excellent sulfur resistance can be determined within a short time, and the sulfur resistance evaluation is also mostly at 200 °C or above, as shown in Table 1. The multicomponent Mn-based catalysts suitable for different industrial requirements are likely to be obtained by doping more kinds of active metals and adjusting appropriate proportion.

H_2O and SO_2 usually work together to aggravate the poisoning effect of the catalyst. However, researchers have found some different phenomena. As shown in Figure 8, at 120 °C, the conversion is close to full recovery after stopping the introduction when SO_2 and H_2O are introduced at the same time. However, the recovery of NO_x conversion for $FeMnO_x$ catalyst is not prominent when SO_2 is introduced alone. Other researchers have found some similar phenomena. As shown in Figure 9, at 110 °C, the NO_x conversion is higher when SO_2 and H_2O are simultaneously introduced. At 220 °C, the NO_x conversion is higher when SO_2 is introduced alone. Different reaction temperatures may have a different influence on the catalyst resistance. At lower temperature, H_2O may have a certain positive effect on the catalyst. The former experimental conditions are 120 °C, 10% H_2O, and 100 ppm of SO_2, and the latter are 110 °C, 9% H_2O, and 100 ppm of SO_2, which proves that H_2O may improve the SO_2 resistance of Mn-based composite catalysts under certain conditions. Studying the positive temperature range of H_2O and the dosage range of poisons is likely to promote the development of Mn-based catalysts for low-temperature NH_3-SCR of NO_x. In addition, calcination temperature, space velocity, and the proportion of active components of composite Mn-based catalysts appear to have an impact on the resistance of the catalyst.

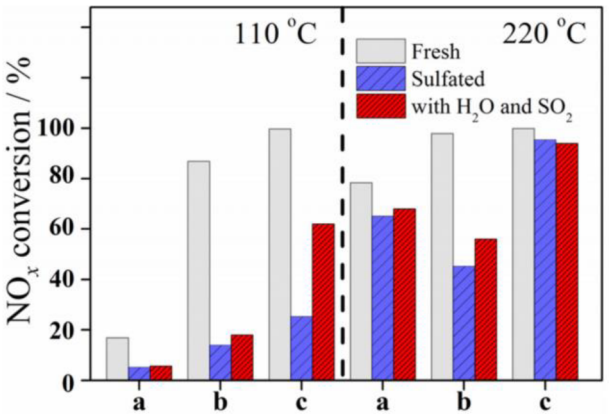

Figure 9. Resistance to SO_2 and combined H_2O and SO_2 over different catalysts (reaction temperature = 110 or 220 °C). Reprinted from ref 69. Copyright 2013 American Chemical Society.

3.2. Carrier. The carrier plays an important role in the catalyst. High redox performance, excellent acidity, and low surface area loss can be obtained with selecting a suitable carrier, thus improving the SO_2 and H_2O resistance of the catalyst.[70,71] The resistance of the Mn-based low-temperature SCR catalysts to H_2O and SO_2 is closely related to the catalyst support. The tolerance of the catalysts can be significantly improved by selecting suitable the metal oxides as supports, as shown in Figure 10. Among them, the Al_2O_3 has high-temperature resistance, excellent mechanical properties, large specific surface area and simple shape control. Obrist et al.[72] studied the NH_3-SCR activity of MnO_x/γ-Al_2O_3 catalysts and the catalysts had high catalytic activity. However, the SO_2 resistance of the Al_2O_3 is poor. For Mn-based low-temperature SCR catalysts, the TiO_2 was proven to be an ideal support.[73,74] Compared with Al_2O_3, TiO_2 has less acidic and more stable physicochemical properties. The findings of Kang et al.[33] confirm that the TiO_2-supported catalyst has higher NO_x conversion compared with the γ-Al_2O_3-supported catalyst when SO_2 is introduced. Active components can be effectively dispersed by the TiO_2 support, and sulfates are easily decomposed on the surface of the TiO_2. Additionally, Smirniotis et al.[75] found that the MnO_x/TiO_2 catalyst had high water resistance. The resistance of the catalyst to SO_2 and H_2O can be significantly improved with the composite metal as a carrier. Xiong et al.[70] found that the doping of Ti increased Ce^{3+} concentration relatively, which inhibited the loss of Mn species on the surface of Mn/CeTi catalysts. Jiang et al.[71]

https://doi.org/10.1021/acsomega.2c06796
ACS Omega 2023, 8, 7262−7278

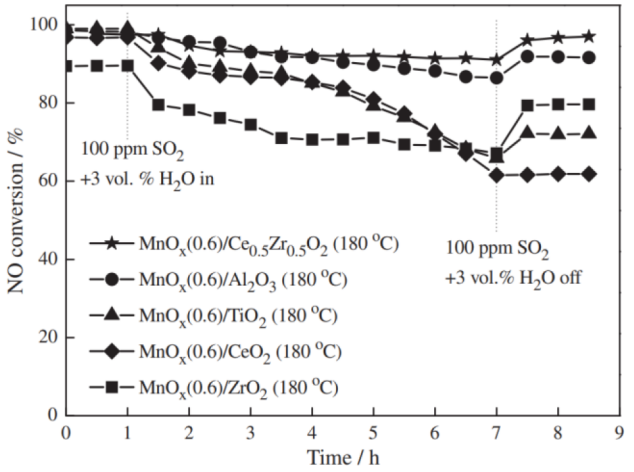

Figure 10. Influence of combined H_2O and SO_2 on NO_x conversion of the catalyst using different carriers(Reaction conditions: [NO] = [NH_3] = 0.06%, [H_2O] = 3%, [SO_2] = 100 ppm, [O_2] = 3%, N_2 to balance, GHSV = 30,000 h^{-1}; reaction temperature = 180 °C. Reprinted with permission from ref 76. Copyright 2014 Elsevier.

found that Zr modification on the Fe-Mn/Ti-$Zr_{0.03}$ catalyst weakened the effect of SO_2 on NO_2 and nitric acid. Jia et al.[32] prepared a series of MnO_x/$ZryTi_{1-y}O_2$ catalysts with different Zr/Ti ratios. The catalysts exhibited excellent water resistance and sulfur resistance at 200 °C. Shen et al.[76] found that the NO conversion of $MnO_{x(0.6)}/Ce_{0.5}Zr_{0.5}O_2$ catalysts remained above 90% after 5 h of reaction at 180 °C in an atmosphere of 3 vol % H_2O and 100 ppm of SO_2. The combination of the advantages of ZrO_2 and CeO_2 carrier was an important reason to improve the resistance to SO_2 and H_2O of the catalysts. Catalyst stability is likely to be further improved by selecting a suitable support combined with a variety of doped active metals. The performance of CeO_x-based capturing SO_x is excellent.[77] Sulfate stability can be reduced with the TiO_2, which is consistent with the previous section on accelerating sulfate decomposition by the Ce and Sn. The stability of sulfate is likely to be further reduced by using TiO_2 as a carrier and the catalyst may decompose at lower temperature to meet industrial low-temperature demand. The number of species for intermediate adsorption can be increased with the composite metal carriers. The species of intermediate adsorption can be also increased with the doped additives. Combining these strategies, the demand of the intermediate adsorbed species in the SCR reaction after poisoning may be still met.

Moreover, the catalyst using other carrier also has excellent tolerance. Pourkhalil et al.[78] found the MnO_x/functionalized multiwalled carbon nanotube (FMWNT) catalyst had excellent resistance to H_2O and SO_2. At 200 °C and 30,000 h^{-1} space velocity, NO_x conversion only decreased by 5% when 2.5 vol % H_2O and 100 ppm of SO_2 were introduced for 6 h. Molecular sieves have a unique mesoporous structure and large specific surface area. Nowadays, the field of molecular sieves involves research of NO and SO_2 gases. Molecular sieves are used to simultaneously adsorb NO and SO_2 to removing the two pollutants. Deng et al.[79] prepared a variety of ion-exchanged molecular sieves and found that K-NaX molecular sieves had the best effect on simultaneously adsorbing NO and SO_2. Yi et al.[80] studied the coadsorption of SO_2 and NO by NaY, NaX, and CaA molecular sieves and found that the stronger the polarity, the better the adsorption capacity of molecular sieves. The molecular sieve has a regular pore structure and molecular sieve screening characteristics. The NO, NH_3, and SO_2 are likely to be separated due to the screening characteristics. The contact between SO_2 and low-temperature SCR catalyst is likely to be reduced thus fundamentally reducing the toxic effect of SO_2 on low-temperature SCR catalyst.

3.3. Load Type. Mn-based supported catalysts have made some progress. High redox performance, low surface area loss, and excellent acidity can be obtained with the combination of metal modification and support, thus improving the SO_2 and H_2O resistance of the catalyst.[35,38,44,81,82] The metal oxide, the molecular sieve supports, and the carbon-based supports summarized in the previous section are mainly contained in the carrier. Among metal oxide supports, the TiO_2 is widely used, while the molecular sieve and carbon-based ones have a wide variety and flexible choices. Doping active metals and selecting suitable carriers are beneficial for improving sulfur resistance and water resistance of the catalyst. Among them, the most doped elements are Ce and Fe. The catalysts doped with Ce had excellent sulfur resistance and water resistance.[83,84] Jin et al.[81] found that doped Ce was beneficial for reducing thermal stability of NH_4HSO_4 on the catalyst surface, as shown in Figure 11. This is also confirmed by Liu et al.,[82] who prepared a Ce-Cu-Mn/SAPO-34 catalyst. Moreover, the Ce protects the main active components from being sulfurized, as shown in Figure 12. The supported catalyst-doped Ce not only has excellent sulfur resistance but also achieves remarkable regeneration. As shown in Figure 11, the activity of the Ce-modified catalyst is mostly restored after washing and regeneration. Fe is a promising Mn-based catalyst dopant. Qi et al.[39] prepared Fe-Mn/TiO_2 and found the formation rate of sulfate species on the catalyst surface could be reduced with doped Fe. Li et al.[38] confirmed that the generation of Mn sulfate and ammonium sulfate can be significantly alleviated with doped Fe, thus improving the sulfur resistance of Mn/

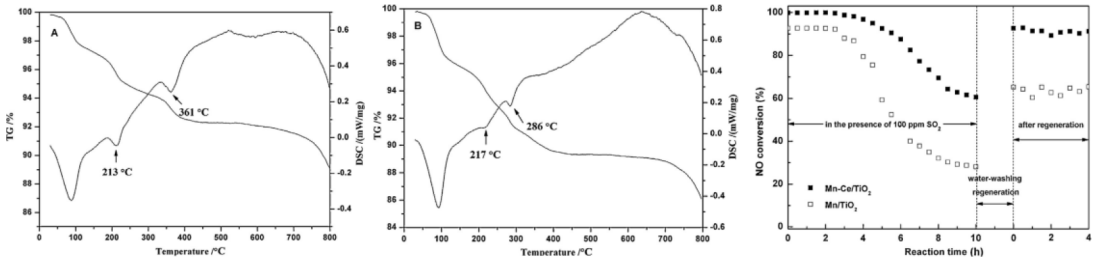

Figure 11. TG and DSC curves of NH_4HSO_4 deposited on Mn/TiO_2(A) and Mn-Ce/TiO_2(B) catalysts and The resistance to SO_2 over Mn/TiO_2 and Mn-Ce/TiO_2 at 150 °C ([NH_3] = [NO] = 800 ppm, [O_2] = 3%, [SO_2] = 100 ppm, [H_2O] = 3 vol %, N_2 to balance, GHSV = 40,000 h^{-1}). Reprinted with permission from ref 81. Copyright 2014 Elsevier.

https://doi.org/10.1021/acsomega.2c06796
ACS Omega 2023, 8, 7262−7278

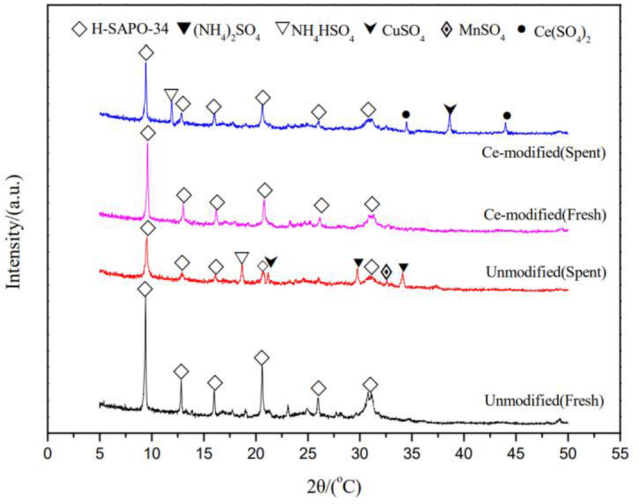

Figure 12. XRD pattern of 2% Ce-modified catalyst after SO_2 poisoning. Reprinted with permission from ref 82. Copyright 2019 MDPI.

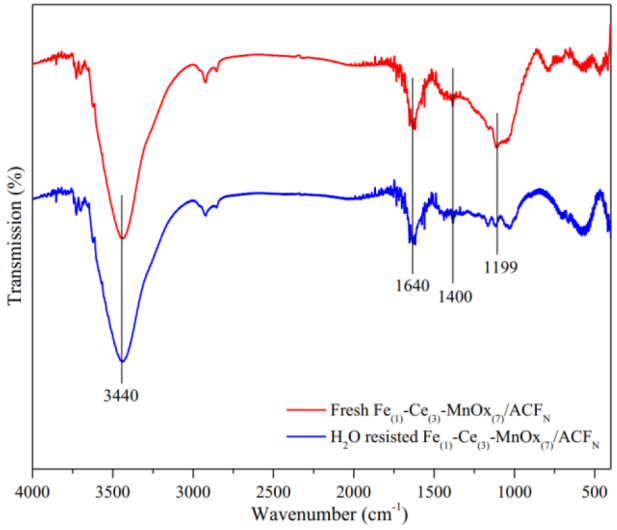

Figure 13. Fourier transform infrared spectra of the fresh and H_2O-resisted $Fe_{(1)}$-$Ce_{(3)}$-$MnO_{x(7)}$/ACFN catalyst. Reprinted with permission from ref 43. Copyright 2019 Springer Nature.

TiO_2 catalysts. Wang et al.[85] prepared a series of Fe-Mn/Al_2O_3 catalysts and found that the catalysts also had a certain tolerance to water and sulfur dioxide after doping Fe. Ce and Fe are commonly used as Mn-based catalyst dopants. Ce, Fe, and Mn ternary composite metal Mn-based catalysts have been widely studied. Cao et al.[40] doped Fe into Mn-Ce/γ-Al_2O_3 to prepare Fe-Mn-Ce/γ-Al_2O_3 catalysts. The FeMnCe/γ-Al_2O_3 catalysts had the excellent resistance to H_2O and SO_2. Shen et al.[41] doped Fe into Mn-Ce/TiO_2 catalysts and obtained a series of Fe-Mn-Ce/TiO_2 catalysts. The FeMnCe/TiO_2 catalysts had excellent resistance to H_2O and SO_2. Shen et al.[86] compared the sulfur resistance of the (Fe,Cu,V)-MnO_x-CeO_x/ACF(activated carbon fiber) catalyst under the atmosphere of 100 ppm of SO_2. The FeMnCe/ACF material had remarkable SO_2 resistance. Gu et al.[43] successfully prepared MnO_x/ACF_N (the rayon-based ACF pretreated with 40 wt % HNO_3 solution), Ce-MnO_x/ACF_N, and Fe-Ce−MnO_x/ACF_N catalysts by ultrasonic impregnation method. The interaction between Mn, Ce, and Fe made the catalysts have excellent water resistance. As shown in Figure 13, the change in the 1199 cm^{-1} band before and after the introduction of H_2O confirms that there was competitive adsorption of NH_3 and H_2O on L acid. The change in the 1400 cm^{-1} band confirmed that the interaction between H_2O and B acid was weaken with Fe-Ce-MnO_x/ACF_N. Mn/TiO_2 and Mn-Nb/TiO_2 catalysts were prepared by Sun et al.[87] The Mn-Nb/TiO_2 catalysts showed outstanding SO_2 resistance. The possible reason was that more NO_2 was formed on the surface of the Mn-Nb/TiO_2 catalyst. Li et al.[88] doped Ho into Mn-Ce-O/TiO_2 catalysts by impregnation method and found that the excellent sulfur resistance and water resistance of the Ho-Mn-Ce-O/TiO_2 catalysts were attributed to the increase of specific surface area, surface O_α, and Mn^{4+}/Mn^{3+}. Jiang et al.[44] modified Mn-Ce-O/AC (activated carbon) catalyst with V_2O_5. Doped V effectively inhibits the formation of ammonium salt and protects main active components, as shown in Figure 14. Chen et al.[89] doped Zr, Co, or Ni into Mn/BC (biochar) catalysts by the impregnation method. The materials doped with Zr had the best sulfur and water resistance. Liu et al.[35] prepared MnO_x/TiO_2 catalysts modified by Eu, and TGA showed sulfate deposition was decreased with doped Eu. The adsorption peak of NO_2 and NH_4^+ is retained with doped Eu and the intensity of sulfate on the surface of MnEu/TiO_2 is lower than that of Mn/TiO_2, as shown in Figure 15. Liu et al.[37] prepared a series of Mn-Sm/TiO_2 catalysts by adding different amounts of Sm elements. The catalyst-doped Sm can inhibit the formation of metal sulfate and the oxidation of SO_2 to SO_3, as shown in Figure 16. Wu et al.[90] doped respectively Fe, W, and Mo into MnO_x/TiO_2 catalyst. The W had better sulfur tolerance. Yang et al.[42] prepared the MnO_x-CeO_2/graphene catalyst doped with noble metals by hydrothermal method. Specific surface area, Mn^{4+}, chemically adsorbed oxygen, and acid sites were increased with the catalyst-doped Pd, thus enhancing SO_2 poisoning resistance. Song et al.[91] synthesized a series of Cu-Mn-SSZ-13 catalysts by exchanging manganese and copper. The catalysts doped with Cu had excellent hydrothermal stability. Zhang et al.[92] prepared Co-Mn-ZSM-5 catalyst by Co and Mn coimpregnating ZSM-5. Under the condition of 100 ppm of SO_2, the NO_x conversion only decreased by 20% at 150 °C. To sum up, the activity, sulfur resistance, and water resistance of supported catalysts are frequently higher than the unsupported catalysts. The Fe, Ce, Eu, Co, Sm, and Cu have excellent sulfur resistance or water resistance in both unsupported and supported catalysts. Both unsupported and supported catalysts appear to have the similar strategies of sulfur resistance. The Eu can enhance the adsorption of intermediate species, and the oxidation of SO_2 to SO_3 can be inhibited with the Sm-modified catalyst. The Ce and V can be used as sacrificial agents to protect the main active components. Moreover, the stability of the ammonium salt can be reduced with doped Ce. The interaction among Mn, Ce, and Fe can makes catalyst keep excellent sulfur resistance or water resistance under different supports, which proves that Fe, Mn, and Ce composite metal catalysts may have the excellent performance independent of supports. And the performance of unloaded FeMnCe catalysts is excellent. Additionally, the Mn-Ce/TiO_2 catalyst-doped Ce has excellent regeneration. The research on catalyst regeneration and recycling is likely to improve catalyst life and reduce industrial cost.

https://doi.org/10.1021/acsomega.2c06796
ACS Omega 2023, 8, 7262−7278

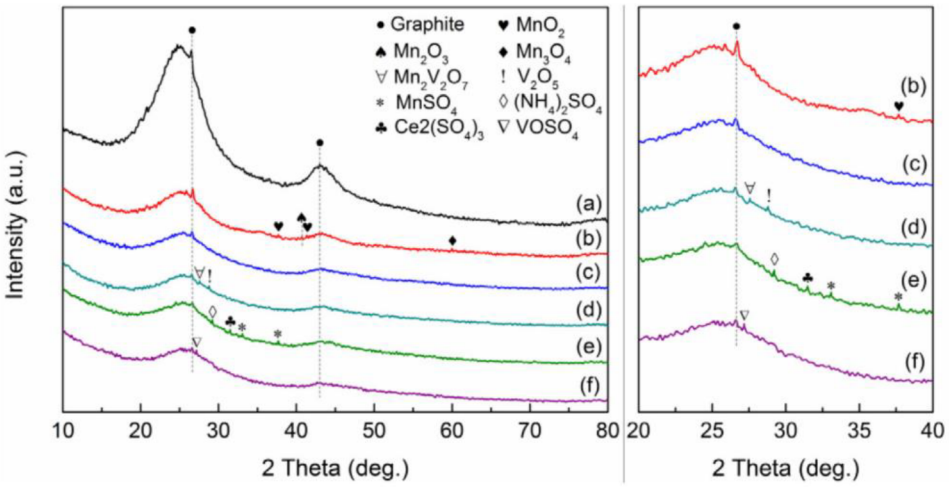

Figure 14. XRD patterns of different catalysts: (a) AC, (b) Mn/AC, (c) Mn-$Ce_{(0.4)}$/AC, (d) Mn-$Ce_{(0.4)}$-V/AC, (e) Mn-$Ce_{(0.4)}$/AC-S, and (f) Mn-$Ce_{(0.4)}$-V/AC-S. The right corresponding to the higher resolution diffraction peaks in 20−40°. Reprinted with permission from ref 44. Copyright 2019 Elsevier.

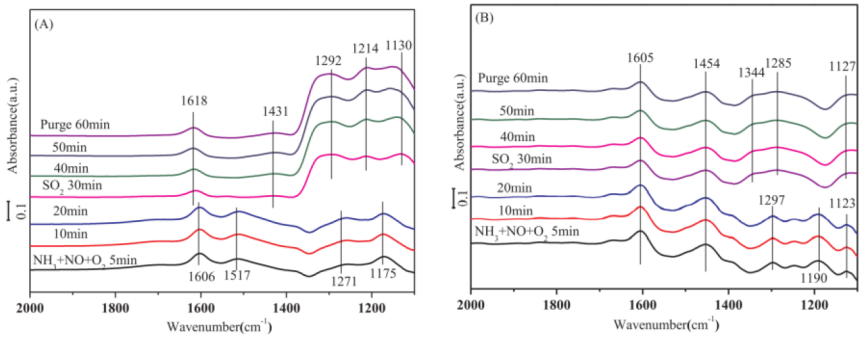

Figure 15. SO_2 adsorption DRIFT spectra for (A) Mn/TiO_2 and (B) $MnEu/TiO_2$ catalysts under the SCR reactions (500 ppm of NH_3 + 500 ppm of NO + 5% O_2, balance to N_2, 100 ppm of SO_2 (when used)) at 150 °C. Reprinted with permission from ref 35. Copyright 2018 Elsevier.

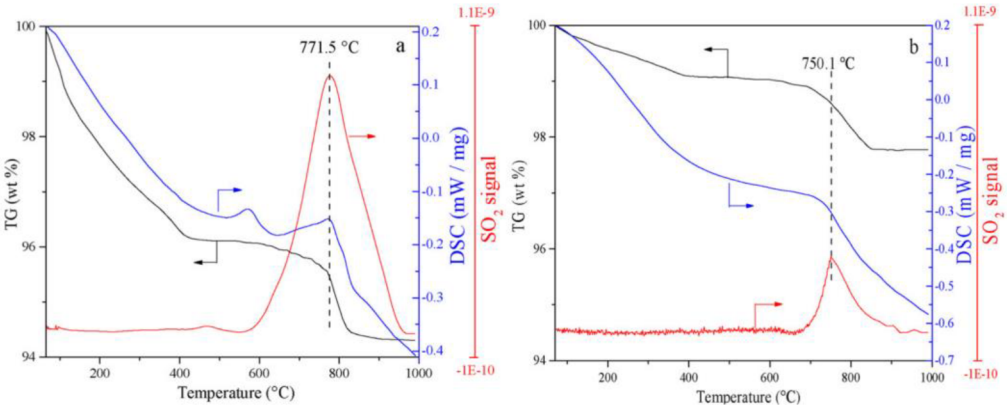

Figure 16. TG-DSC-MS curves of $20Mn/TiO_2$ (a) and 20Mn-10Sm/TiO_2 (b) catalysts pretreated by H_2O and SO_2 during SCR reaction. Reprinted with permission from ref 37. Copyright 2020 Elsevier.

3.4. Special Structure Type. *3.4.1. Core−Shell Structure Type.* Core−shell structure combines inner and outer layers to achieve desired effect. The outer layer is mainly used as a sacrificial layer, inhibits SO_2 adsorption, slows down the formation of sulfate substances and protects main active components of the inner layer. The CeO_2 shells of high redox performance were beneficial for capturing SO_2.[46] Fe_2O_3 shell was beneficial for enhancing the alkalinity of the catalyst surface.[47] CNT-supported core−shell structure was widely studied. Zhang et al.[48] prepared a core−shell SCR catalyst mesoTiO$_2$@MnCe/CNTs with mesoporous TiO_2 as the shell and CNT-loaded MnO_x-CeO_x nanoparticles as the core. The adsorption of SO_2 and the generation of sulfate could be inhibited with the mesoporous TiO_2 shell of the catalyst. The research of Zhang et al.[93] also confirmed this point. Mesoporous TiO_2 layer was coated on MnO_x and CeO_x nanoparticles supported by carbon nanotubes, thus improving the SO_2 poisoning resistance of the catalyst. Cai et al.[47] got a

https://doi.org/10.1021/acsomega.2c06796
ACS Omega 2023, 8, 7262−7278

similar conclusion. The formation of sulfate on the surface of catalysts could also be effectively inhibited with Fe_2O_3 shell. Fang et al.[45] prepared nf-MnO_x@CNT catalysts with core−shell structure by chemical deposition. Compared with MnO_x/CNT and MnO_x/TiO_2 catalysts, nf-MnO_x@CNT catalyst showed excellent H_2O resistance. Additionally, Liu et al.[94] prepared MnO_2@$NiCO_2O_4$ core−shell nanorods with nickel foam as carrier. The Ni−Co nanorods had high specific surface area and there was an excellent synergy among Ni, Co, and Mn oxides, thus promoting the excellent low-temperature activity and H_2O resistance of the catalyst. Li et al.[46] prepared core−shell CeO_2−MnO_x bimetallic oxide. The catalysts had relatively excellent SO_2 resistance. In the presence of SO_2, the high activity of the catalyst can be only maintained with the method doping metal for a limited time. The sulfur resistance time of the catalyst can be relatively prolonged with the protective shell method. However, the activation temperature is relatively high. In order to find a catalyst with excellent denitration activity and excellent sulfur resistance at low temperature, the fresh strategy based on the two methods is necessary to further research. In the core−shell structure, SO_2 adsorption can be inhibited with the mesoporous TiO_2 layer, sulfate formation can be inhibited with the Fe_2O_3 shell, and the shell layer plays an important role in improving SO_2 resistance. Combined with the research of the catalyst-doped metal, other metal oxides or composite metal oxides can be considered as shell layers to further improving the performance of Mn-based catalysts.

MnO_x nanoparticles are surrounded by a layer of crystalline CeO_2 shell, as shown in Figure 17. It can be found from Figure

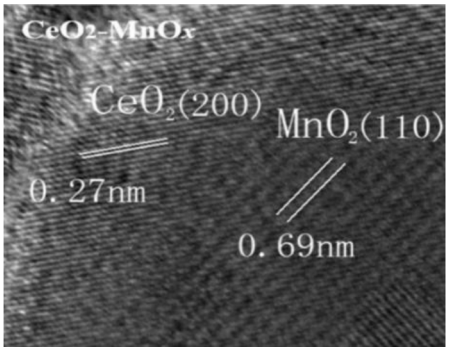

Figure 17. High-resolution transmission electron microscopy image of the CeO_2−MnO_x. Reprinted from ref 95. Copyright 2017 American Chemical Society.

18 that the TiO_2 layer is wrapped with Mn Ce/CNTs. Fe, Mn and C are listed from outside to inside (Figure 19). The core−shell structure had distinct layers, and the outer layer was designed to protect the inner layer. On account of the layering, each layer can be independently designed. The inner and outer layers were designed combined with the metal doping modification. The overall stability of the catalyst can be mainly improved with the outer layer. And the catalyst activity was mainly increased with the inner layer, which can improve the catalyst performance to the greatest extent. If the catalyst activity was satisfied, metal doping in the inner layer was conducive to improving the tolerance of the catalyst, which may improve the tolerance of the catalyst to meet the requirements of industrial application.

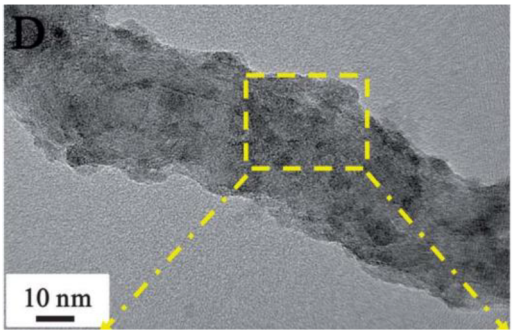

Figure 18. Transmission electron microscopy image of meso-TiO_2@MnCe/CNTs. Reprinted with permission from ref 48. Copyright 2013 Royal Society of Chemistry.

3.4.2. Other Special Structure Types. The hollow structure improves the resistance to SO_2 and H_2O. The probable reason is that the active ingredients are uniformly dispersed in the nanotubes (Figure 20). Li et al.[96] obtained a composite MnO_x-CeO_2 nano-oxide with a hollow tubular structure by an interfacial redox reaction. Excellent sulfur resistance and water resistance were obtained, which might be related to the unique hollow tubular structure. Jiang et al.[34] prepared the Mn-MOF-74 catalyst with a hollow spherical structure and found that the NO conversion efficiency of Mn-MOF-74 could be kept at 85% in the presence of 5% H_2O and 100 ppm of SO_2. Moreover, other special structures also have certain sulfur resistance and water resistance. Gao et al.[97] obtained highly sulfur-resistant spinel nanosheet-structured Mn−Ni catalysts. The high sulfur resistance of the catalysts was attributed to the external tetrahedral configuration protecting the internal Mn active site. Meng et al.[23] prepared a series of $Co_aMn_bO_x$ catalysts. The $Co_7Mn_3O_x$ catalysts with the spinel structure promoted the resistance to SO_2 and H_2O. Gao et al.[49] successfully prepared two Mn/CeO_2 catalysts by impregnating CeO_2 microspheres and CeO_2 micron rods with Mn. The Mn/CeO_2-MSs catalyst had excellent SO_2 and H_2O resistance. Zhang et al.[98] found that the $Mn_xCo_{1-x}O_4$ catalysts with nanocages had better SO_2 and H_2O resistance than the $Mn_xCo_{1-x}O_4$ catalysts with nanoparticles. The probable reason is that nanocages of the $Mn_xCo_{1-x}O_4$ catalysts enhanced the interaction between MnO_x and CoO_x. Additionally, adjusting the pore structure of catalysts can achieve a dynamic balance between the formation and decomposition of ammonium sulfate on the catalyst's surface. Then, the catalysts can reduce the degree of ammonium sulfate deposition on the surface. Yu et al.[55] found that Mn-based catalysts showed excellent sulfur resistance when pore size was 2−50 nm. The $(NH_4)_2SO_4$ specie achieved the balance of formation and decomposition in mesoporous channels. The larger pore structure was beneficial for the decomposition of the ammonium salts on the catalyst's surface,[59,99,100] as shown in Figure 21.

3.5. Preparation Method. The preparation method has a significant effect on the structure of the catalyst, and the physical form structure of the catalyst is closely related to its physicochemical properties. Moreover, the preparation method is critical in determining the excellent dispersion of active components and particle size. Accordingly, the preparation method can be optimized for the catalyst's performance. Different preparation methods obtain different tolerance of the catalysts, as shown in Figure 22. Sol−gel and surfactant template methods play a more significant role than the

https://doi.org/10.1021/acsomega.2c06796
ACS Omega 2023, 8, 7262−7278

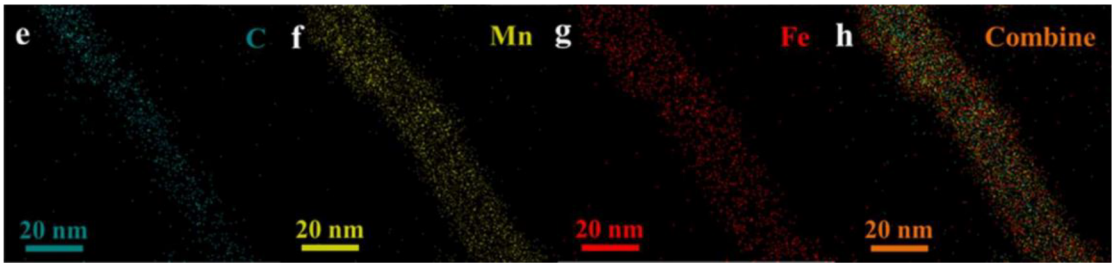

Figure 19. Elemental mapping images of Fe@Mn@CNTs. Reprinted with permission from ref 47. Copyright 2016 Royal Society of Chemistry.

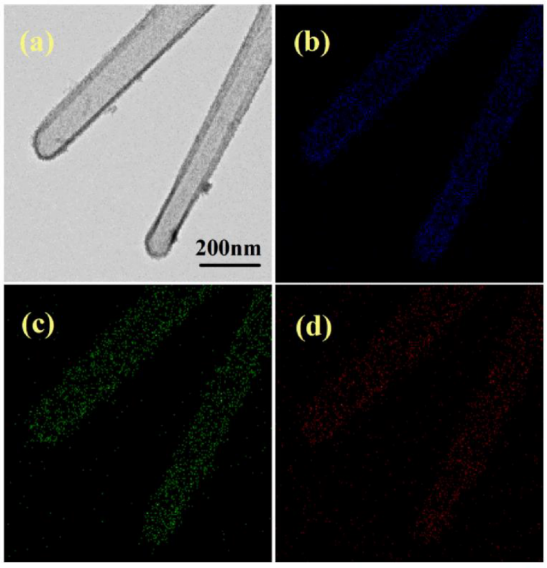

Figure 20. Scanning transmission electron microscopy (a) image of MnO_x-CeO_2 nano-oxide and energy-dispersive X-ray spectroscopy of Mn (b), Ce (c), and O (d). Reprinted with permission from ref 96. Copyright 2018 Elsevier.

coprecipitation and impregnation methods in resisting SO_2 and H_2O. The MnO_x/TiO_2 catalyst was prepared by Jiang et al.[101] using the sol−gel way. The way showed better SO_2 tolerance than the MnO_x/TiO_2 catalyst prepared by the impregnation and coprecipitation methods. Liu et al.[62] compared the performance of the MnO_x-CeO_2 catalyst prepared by surfactant template and conventional coprecipitation method. At a space velocity ratio of 64,000 h^{-1} and 150−200 °C, the MnO_x-CeO_2 catalyst prepared by the surfactant template method could keep the NO_x conversion above 90% in the atmosphere of 5 vol % H_2O and 50 ppm of SO_2. Yu et al.[55] reported a mesoporous MnO_2-Fe_2O_3-CeO_2-TiO_2 catalyst prepared by the sol−gel method, which had higher resistance to SO_2 and H_2O than the conventional impregnation method. The improvement of traditional preparation methods has achieved some progress. Yao et al.[102] prepared MnO_x/CeO_2 nanomaterials by adjusting the solvent. The catalyst prepared by $(HCOOH)_2$ solution as solvent showed excellent sulfur and water resistance. Zhang et al.[103] loaded MnO_x and CeO_2 on the CNTs using an auxiliary reflux route. Compared with the traditional preparation process, the method had certain advantages in sulfur and water resistance. Sheng et al.[104] used a novel coprecipitation method to synthesize the Mn-Ce/TiO_2 catalyst. The catalyst had stable SO_2 resistance. Shi et al.[105] systematically compared the SO_2 tolerance of Mn/TiO_2 prepared by the conventional sol−gel method and layered mesoporous Mn/TiO_2 catalysts prepared by the Planck F127 assisted sol−gel method. After adding 30 ppm of SO_2 to inlet flue gas at 120 °C, the NO conversion rate of ordinary Mn/TiO_2 drops sharply from 57 to 15% within 6 h, while the NO conversion rate of HM Mn/TiO_2 remains above 84%. Zou et al.[106] prepared Mn-Fe/ZSM-5 catalysts by coprecipitation and precipitation−chemical vapor deposition methods. The Mn-Fe/ZSM-5 catalyst obtained by method B had higher SO_2 resistance. The possible reason was that the decomposition of sulfate was faster for the Mn-Fe/ZSM-5 catalyst prepared by this method. The unique preparation methods can obtain the catalysts with the better effect of treating H_2O alone to meet some industrial scenes. Huang et al.[107] found that the SCR activity of the MnO_2-Co_3O_4/TiO_2 catalyst was hardly affected by H_2O. The probable reason was that the MnO_2-Co_3O_4/TiO_2 catalyst obtained nanorod heterostructure using the photocatalyst method.

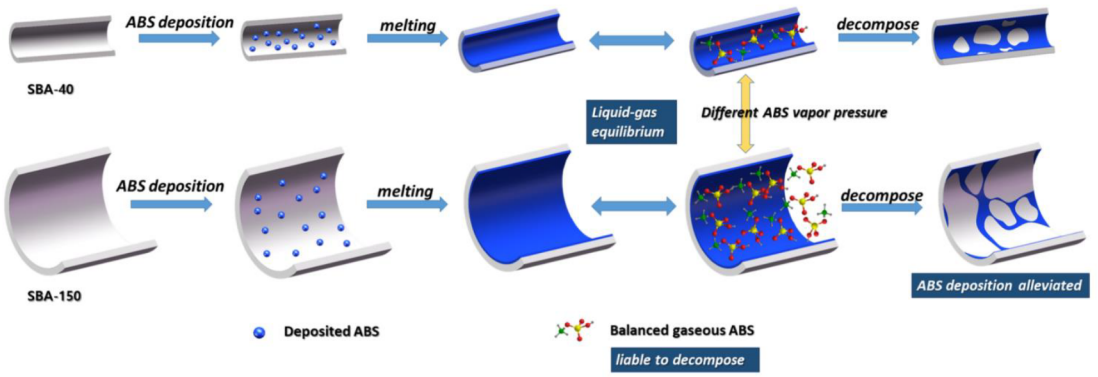

Figure 21. Decomposition of ammonium salts on the catalyst with different pore sizes. Reprinted from ref 100. Copyright 2019 American Chemical Society.

https://doi.org/10.1021/acsomega.2c06796
ACS Omega 2023, 8, 7262−7278

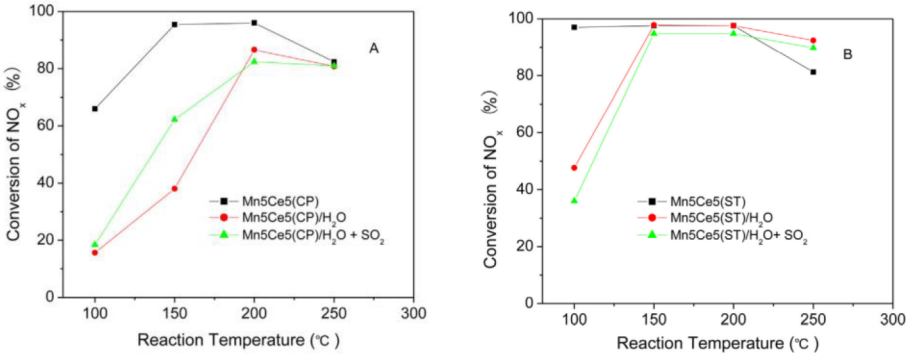

Figure 22. Influence of H_2O and SO_2 on NO_x conversion of the catalyst using different preparation methods: (A) the conventional coprecipitation method and (B) the surfactant-template method (reaction conditions: [NO] = [NH_3] = 0.05%, [H_2O] = 5%, [SO_2] = 50 ppm, [O_2] = 5%, N_2 to balance, GHSV = 64,000 h^{-1}). Reprinted with permission from ref 62. Copyright 2013 Elsevier.

4. CONCLUSIONS AND PROSPECTS

For low-temperature denitration catalyst, the strong inactivation effect of H_2O and SO_2 on the active metal of catalyst is the main reason for the NH_3-SCR, which severely reduces the catalytic efficiency and performance in many fields. Thus, an ideal catalyst is required to possess not only a strong adsorption for NO_x but also the ability to propel denitration conversion efficient, which is expected as the ultimate remedy for suppressing the catalyst poisoning from the deactivation with H_2O and SO_2. Most of Mn-based catalytic materials have been widely used and investigated in the de-NO_x industry, the catalysts promoting denitration based compound conversion in traditional chemical reactions may provide a new way to high-efficiency catalytically promote conversion in the comprehensive denitration industry. At the current stage, identifying the catalytic mechanism is expected to provide a design principle for the catalytic denitration conversion. Thus, the mechanisms of H_2O and SO_2 poisoning on NH_3-SCR catalysts and performance of Mn-based low-temperature denitration catalysts are greatly needed to help understand the conversion process from NO_x to N_2.

In this review, some key points for high-efficiency catalyst design for the reaction of denitration conversion are summarized:

(1) Mn-based catalytic materials have a potential application value in large-scale industrial application, which consist of cement, glass, metallurgy, petrochemical catalytic cracking, chemical industry, waste incineration and other fields, attributing to the superior low-temperature catalytic activity, nontoxicity and low cost. To achieve industrial expectations, Mn based low-temperature SCR catalyst not only needs to have high denitration efficiency, thermal stability and good N_2 selectivity, but also have strong anti-H_2O and SO_2 performance. Therefore, it is very important to carry out research to improve its relevant performance and clarify its relevant mechanism, especially the Manganese−Cerium catalyst for sulfur and water resistance at low temperature.

(2) The deactivation mechanism of Mn-based denitration catalyst under SO_2 was systematically identified. The passivated contact reaction focuses on the formation of ammonium sulfate and metal sulfate on the surface of the catalyst in NH_3-SCR, which will block the active sites and causes deactivation, which generating the competitive adsorption SO_2, reducing the formation of active intermediates and causing deactivation. Intrinsically, part of SO_2 was catalytically oxidized into SO_3 by the active components in denitration catalyst, and then the continuous reaction was triggered between SO_3 with escaping NH_3 and H_2O to producing fine particles of ammonium sulfate, and also the coterminous reaction with metal oxides in fly ash was formed to producing sulfate particles, all of that will cover the active sites of the catalyst resulting in blockage and deactivation of the catalyst eventually; SO_2 can also react with metal oxides on the catalyst surface to generate metal sulfate, which will adsorb on the surface of catalyst and hinder the subsequent denitration reaction. According to the deactivation mechanism of catalyst, it is found that the sulfur resistance of catalyst at low temperature can be improved by reducing SO_2 oxidation and protecting active sites. There are mature methods including metal modification, construction of special core−shell structure, selection of better supports and acidification catalysts.

(3) Although the reported methods have been proved to be helpful to improve the anti-SO_2 poisoning performance of denitration catalyst, the mechanism of anti-SO_2 poisoning under complex working conditions is still unclear. It is necessary to further study the anti-SO_2 poisoning mechanism of NH_3-SCR denitration catalyst, especially in the following aspects: (1) properly adjust the acidity and introduce a protective layer to inhibiting SO_2 adsorption; (2) properly reduce the oxidation of active sites to suppression the oxidation of SO_2; (3) realize the dynamic balance between the formation and decomposition of ammonium sulfate, inhibit its deposition on the catalyst surface, and promote the decomposition of generated sulfate.

In summary, the low-temperature denitration activity and stability of denitration catalyst with the impact of SO_2 is still the focus of future research. It is necessary to develop novel and efficient modification strategy on anti-SO_2 poisoning catalyst to further improve the catalytic performance of NH_3-SCR denitration in low-temperature. It is the future research orientation of low-temperature denitration catalyst regeneration to match the online thermal regeneration and thermal analysis device in the low-temperature denitration to realize online regeneration catalyst.

AUTHOR INFORMATION

Corresponding Author

Xuetao Wang − *Department of Energy and Power Engineering, Henan University of Science and Technology, Luoyang 471003, China;* orcid.org/0000-0002-5375-0695; Email: wangxuetao@haust.edu.cn

https://doi.org/10.1021/acsomega.2c06796
ACS Omega 2023, 8, 7262−7278

Authors

Jungang Tang − *Department of Energy and Power Engineering, Henan University of Science and Technology, Luoyang 471003, China*

Haojie Li − *Department of Energy and Power Engineering, Henan University of Science and Technology, Luoyang 471003, China;* orcid.org/0000-0002-6115-2409

Lili Xing − *Department of Energy and Power Engineering, Henan University of Science and Technology, Luoyang 471003, China;* orcid.org/0000-0003-2099-8472

Mengjie Liu − *Department of Energy and Power Engineering, Henan University of Science and Technology, Luoyang 471003, China*

Complete contact information is available at: https://pubs.acs.org/10.1021/acsomega.2c06796

Notes

The authors declare no competing financial interest.

■ ACKNOWLEDGMENTS

The authors gratefully acknowledged financial project supported by National Natural Science Foundation of China (50806020); Henan Science and Technology Innovation Talent Program (Outstanding Youth) (114100510010); Science and Technology Project of Science and Technology Department of Henan Province (152102210280).

■ REFERENCES

(1) Fang, Z.; Lin, T.; Xu, H.; Wu, G.; Sun, M.; Chen, Y. Novel promoting effects of cerium on the activities of NO_x reduction by NH_3 over TiO_2-SiO_2-WO_3 monolith catalysts. *Journal of Rare Earths* **2014**, *32*, 952−959.

(2) Busca, G.; Lietti, L.; Ramis, G.; Berti, F. Chemical and mechanistic aspects of the selective catalytic reduction of NO_x by ammonia over oxide catalysts: A review. *Appl. Catal. B* **1998**, *18* (1−2), 1−36.

(3) Kantcheva, M. Identification, Stability, and Reactivity of NO_x Species Adsorbed on Titania-Supported Manganese Catalysts. *J. Catal.* **2001**, *204* (2), 479−494.

(4) Gao, F.; Tang, X.; Yi, H.; Zhao, S.; Li, C.; Li, J.; Shi, Y.; Meng, X. A Review on Selective Catalytic Reduction of NO_x by NH_3 over Mn−Based Catalysts at Low Temperatures: Catalysts, Mechanisms, Kinetics and DFT Calculations. *Catalysts* **2017**, *7* (7), 199.

(5) Liu, C.; Shi, J.-W.; Gao, C.; Niu, C. Manganese oxide-based catalysts for low-temperature selective catalytic reduction of NO_x with NH_3: A review. *Appl. Catal. A* **2016**, *522*, 54−69.

(6) Liu, F.; Shan, W.; Shi, X.; Zhang, C.; He, H. Research Progress in Vanadium-Free Catalysts for the Selective Catalytic Reduction of NO with NH_3. *Chinese Journal of Catalysis* **2013**, *32* (7), 1113−1128.

(7) Shan, W.; Liu, F.; Yu, Y.; He, H. The use of ceria for the selective catalytic reduction of NO_x with NH_3. *Chinese Journal of Catalysis* **2014**, *35* (8), 1251−1259.

(8) Shan, W.; Song, H. Catalysts for the selective catalytic reduction of NO_x with NH_3 at low temperature. *Catalysis Science & Technology* **2015**, *5*, 4280−4288.

(9) Zhang, S.; Zhang, B.; Liu, B.; Sun, S. A review of Mn-containing oxide catalysts for low temperature selective catalytic reduction of NO_x with NH_3: reaction mechanism and catalyst deactivation. *Rsc Advances* **2017**, *7* (42), 26226−26242.

(10) Si, M.; Shen, B.; Adwek, G.; Xiong, L.; Liu, L.; Yuan, P.; Gao, H.; Liang, C.; Guo, Q. Review on the NO removal from flue gas by oxidation methods. *Journal of Environmental Sciences* **2021**, *101*, 49−71.

(11) Xu, J.; Chen, G.; Guo, F.; Xie, J. Development of wide-temperature vanadium-based catalysts for selective catalytic reducing of NO_x with ammonia: Review. *Chemical Engineering Journal* **2018**, *353*, 507−518.

(12) Kapteijn, F.; Singoredjo, L.; Andreini, A.; Moulijn, J. A. Activity and selectivity of pure manganese oxides in the selective catalytic reduction of nitric oxide with ammonia - ScienceDirect. *Appl. Catal. B* **1994**, *3* (2−3), 173−189.

(13) Kang, M.; Park, E. D.; Kim, J. M.; Yie, J. E. Manganese oxide catalysts for NO_x reduction with NH_3 at low temperatures. *Appl. Catal. A* **2007**, *327* (2), 261−269.

(14) Tang, X.; Hao, J.; Xu, W.; Li, J. Low temperature selective catalytic reduction of NO_x with NH_3 over amorphous MnO_x catalysts prepared by three methods. *Catal. Commun.* **2007**, *8* (3), 329−334.

(15) Tian, W.; Yang, H.; Fan, X.; Zhang, X. Catalytic reduction of NO_x with NH_3 over different-shaped MnO_2 at low temperature. *Journal of hazardous materials* **2011**, *188*, 105−109.

(16) Zhang, X.; Lv, S.; Zhang, X.; Xiao, K.; Wu, X. Improvement of the activity and SO_2 tolerance of Sb-modified Mn/PG catalysts for NH_3-SCR at a low temperature. *Journal of Environmental Sciences* **2021**, *101* (03), 1−15.

(17) Shi, X.; Guo, J.; Shen, T.; Fan, A.; Liu, Y.; Yuan, S. Improvement of NH_3-SCR activity and resistance to SO_2 and H_2O by Ce modified La-Mn perovskite catalyst. *Journal of the Taiwan Institute of Chemical Engineers* **2021**, *126*, 102−111.

(18) Raja, S.; Alphin, M. S.; Sivachandiran, L.; Singh, P.; Damma, D.; Smirniotis, P. G. TiO_2-carbon nanotubes composite supported MnO_x-CuO catalyst for low-temperature NH_3-SCR of NO: Investigation of SO_2 and H_2O tolerance. *Fuel* **2022**, *307*, 121886.

(19) Wang, X.; Zhao, Z.; Xu, Y.; Li, Q. Promoting effect of Ti addition on three-dimensionally ordered macroporous Mn-Ce catalysts for NH_3-SCR reaction: Enhanced N_2 selectivity and remarkable water resistance: Applied Surface Science: A Journal Devoted to the Properties of Interfaces in Relation to the Synthesis and Behaviour of Materials. *Appl. Surf. Sci.* **2021**, *569*, 151047.

(20) Chen, C.; Xie, H.; He, P.; Liu, X.; Yang, C.; Wang, N.; Ge, C. Comparison of low-temperature catalytic activity and H_2O/SO_2 resistance of the Ce-Mn/TiO_2 NH_3-SCR catalysts prepared by the reverse co-precipitation, co-precipitation and impregnation method. *Appl. Surf. Sci.* **2022**, *571*, 151285.

(21) Chen, Z.; Wang, F.; Li, H.; Yang, Q.; Wang, L.; Li, X. Low-Temperature Selective Catalytic Reduction of NO_x with NH_3 over Fe−Mn Mixed-Oxide Catalysts Containing $Fe_3Mn_3O_8$ Phase. *Ind. Eng. Chem. Res.* **2012**, *51* (1), 202−212.

(22) Chen, Z.; Yang, Q.; Li, H.; Li, X.; Wang, L.; Chi Tsang, S. Cr-MnO_x mixed-oxide catalysts for selective catalytic reduction of NO_x with NH_3 at low temperature. *J. Catal.* **2010**, *276* (1), 56−65.

(23) Meng, D.; Xu, Q.; Jiao, Y.; Guo, Y.; Guo, Y.; Wang, L.; Lu, G.; Zhan, W. Spinel structured $Co_aMn_bO_x$ mixed oxide catalyst for the selective catalytic reduction of NO_x with NH_3. *Appl. Catal. B* **2018**, *221*, 652.

(24) Sun, P.; Guo, R.-t.; Liu, S.-m.; Wang, S.-x.; Pan, W.-g.; Li, M.-y. The enhanced performance of MnO_x catalyst for NH_3-SCR reaction by the modification with Eu. *Appl. Catal.* **2017**, *531*, 129.

(25) France, L. J.; Yang, Q.; Li, W.; Chen, Z.; Guang, J.; Guo, D.; Wang, L.; Li, X. Ceria modified $FeMnO_x$-Enhanced performance and sulphur resistance for low-temperature SCR of NO_x. *Appl. Catal. B* **2017**, *206*, 203−215.

(26) Chen, L.; Li, R.; Li, Z.; Yuan, F.; Niu, X.; Zhu, Y. Effect of Ni doping in $Ni_xMn_{1-x}Ti_{10}$ (x = 0.1−0.5) on activity and SO_2 resistance for NH_3-SCR of NO studied with in situ DRIFTS. *Catalysis Science & Technology* **2017**, *7* (15), 3243.

(27) Fang, N.; Guo, J.; Shu, S.; Luo, H.; Chu, Y.; Li, J. Enhancement of low-temperature activity and sulfur resistance of $Fe_{0.3}Mn_{0.5}Zr_{0.2}$ catalyst for NO removal by NH_3-SCR. *Chemical Engineering Journal* **2017**, *325*, 114.

(28) Guo, M.; Zhao, P.; Liu, Q.; Liu, C.; Han, J.; Ji, N.; Song, C.; Ma, D.; Lu, X.; Liang, X.; Li, Z. Improved Low-Temperature Activity and H_2O Resistance of Fe-Doped MnEu Catalysts for NO Removal by NH_3-SCR. *ChemCatChem.* **2019**, *11*, 4954.

(29) Gao, F.; Tang, X.; Yi, H.; Li, J.; Zhao, S.; Wang, J.; Chu, C.; Li, C. Promotional mechanisms of activity and SO_2 tolerance of Co- or Ni-doped MnO_x-CeO_2 catalysts for SCR of NO_x with NH_3 at low temperature. *Chemical Engineering Journal* **2017**, *317*, 20−31.
(30) Tong, Y.; Li, Y.; Li, Z.; Wang, P.; Zhang, Z.; Zhao, X.; Yuan, F.; Zhu, Y. Influence of Sm on the low temperature NH_3-SCR of NO activity and H_2O/SO_2 resistance over the $Sm_aMnNi_2Ti_7O_x$ (a = 0.1, 0.2, 0.3, 0.4) catalysts. *Appl. Catal. A* **2020**, *590*, 117333.
(31) Sun, C.; Liu, H.; Chen, W.; Chen, D.; Yu, S.; Liu, A.; Dong, L.; Feng, S. Insights into the Sm/Zr co-doping effects on N_2 selectivity and SO_2 resistance of a MnO_x-TiO_2 catalyst for the NH_3-SCR reaction. *Chemical Engineering Journal* **2018**, *347*, 27−40.
(32) Jia, B.; Guo, J.; Shu, S.; Fang, N.; Li, J.; Chu, Y. Effects of different Zr/Ti ratios on NH_3−SCR over $MnO_x/Zr_yTi_{1-y}O_2$: Characterization and reaction mechanism - ScienceDirect. *Molecular Catalysis* **2017**, *443*, 25−37.
(33) Kang, M.; Park, J. H.; Choi, J. S.; Park, E. D.; Yie, J. E. Low-temperature catalytic reduction of nitrogen oxides with ammonia over supported manganese oxide catalysts. *Korean Journal of Chemical Engineering* **2007**, *24* (1), 191−195.
(34) Jiang, H.; Wang, Q.; Wang, H.; Chen, Y.; Zhang, M. MOF-74 as an Efficient Catalyst for the Low-Temperature Selective Catalytic Reduction of NO_x with NH_3. *ACS Appl. Mater. Interfaces* **2016**, *8*, 26817.
(35) Liu, J.; Guo, R. T.; Li, M. Y.; Sun, P.; Liu, S. M.; Pan, W. G.; Liu, S. W.; Sun, X. Enhancement of the SO_2 resistance of Mn/TiO_2 SCR catalyst by Eu modification: A mechanism study. *FUEL* **2018**, *223*, 385−393.
(36) Zhang, S.; Zhao, L.; Feng, J.; Luo, X.; Dong, H. Parameter optimization of gas-solid heat transfer process in sinter packed bed based on further exergy analysis. *Chem. Eng. Res. Des.* **2019**, *146*, 499.
(37) Liu, L.; Xu, K.; Su, S.; He, L.; Qing, M.; Chi, H.; Liu, T.; Hu, S.; Wang, Y.; Xiang, J. Efficient Sm modified Mn/TiO_2 catalysts for selective catalytic reduction of NO with NH_3 at low temperature. *Appl. Catal. A* **2020**, *592*, 117413.
(38) Li, F.; Xie, J.; Qi, K.; Gong, P.; He, F. Evaluating the Intermetallic Interaction of Fe or Cu Doped Mn/TiO_2 Catalysts: SCR Activity and Sulfur Tolerance. *Catal. Lett.* **2019**, *149*, 788.
(39) Qi, G.; Yang, R. T. Low-temperature selective catalytic reduction of NO with NH_3 over iron and manganese oxides supported on titania. *Appl. Catal. B* **2003**, *44* (3), 217−225.
(40) Cao, F.; Su, S.; Xiang, J.; Wang, P.; Hu, S.; Sun, L.; Zhang, A. The activity and mechanism study of Fe−Mn−Ce/γ-Al_2O_3 catalyst for low temperature selective catalytic reduction of NO with NH_3. *Fuel* **2015**, *139*, 232−239.
(41) Shen, B.; Liu, T.; Zhao, N.; Yang, X.; Deng, L. Iron-doped Mn-Ce/TiO_2 catalyst for low temperature selective catalytic reduction of NO with NH_3. *J. Environ. Sci.* **2010**, *22*, 1447−1454.
(42) Yang, L.; You, X.; Sheng, Z.; Ma, D.; Yu, D.; Xiao, X.; Wang, S. The promoting effect of noble metal (Rh, Ru, Pt, Pd) doping on the performances of MnO_x−CeO_2/graphene catalysts for the selective catalytic reduction of NO with NH_3 at low temperatures. *New J. Chem.* **2018**, *42*, 11673.
(43) Gu, T.; Gao, F.; Tang, X.; Yi, H.; Zhao, S.; Zaharaddeen, S.; Zhang, R.; Zhuang, R.; Ma, Y. Fe-modified Ce-MnO_x/ACFN catalysts for selective catalytic reduction of NO_x by NH_3 at low-middle temperature. *Environmental Science and Pollution Research* **2019**, *26* (26), 27940−27952.
(44) Jiang, L.; Liu, Q.; Ran, G.; Kong, M.; Ren, S.; Yang, J.; Li, J. V_2O_5-modified Mn-Ce/AC catalyst with high SO_2 tolerance for low-temperature NH_3-SCR of NO. *Chemical Engineering Journal* **2019**, *370*, 810−821.
(45) Fang, C.; Zhang, D.; Cai, S.; Zhang, L.; Huang, L.; Li, H.; Maitarad, P.; Shi, L.; Gao, R.; Zhang, J. Low-temperature selective catalytic reduction of NO with NH_3 over nanoflaky MnO_x on carbon nanotubes in situ prepared via a chemical bath deposition route. *Nanoscale* **2013**, *5* (19), 9199−9207.
(46) Li, S.; Huang, B.; Yu, C. A CeO_2-MnO_x core-shell catalyst for low-temperature NH_3-SCR of NO. *Catal. Commun.* **2017**, *98*, 47−51.
(47) Cai, S.; Hu, H.; Li, H.; Shi, L.; Zhang, D. Design of multi-shell Fe_2O_3@MnO_x@CNTs for the selective catalytic reduction of NO with NH_3: improvement of catalytic activity and SO_2 tolerance. *Nanoscale* **2016**, *8* (6), 3588.
(48) Zhang, L.; Zhang, D.; Zhang, J.; Cai, S.; Fang, C.; Huang, L.; Li, H.; Gao, R.; Shi, L. Design of meso-TiO_2@$MnO_{(x)}$-$CeO_{(x)}$/CNTs with a core-shell structure as $DeNO_{(x)}$ catalysts: promotion of activity, stability and SO_2-tolerance. *Nanoscale* **2013**, *5* (20), 9821.
(49) Gao, G.; Shi, J.-W.; Liu, C.; Gao, C.; Fan, Z.; Niu, C. Mn/CeO_2 catalysts for SCR of NO_x with NH_3: comparative study on the effect of supports on low-temperature catalytic activity. *Appl. Surf. Sci.* **2017**, *411*, 338.
(50) Huo, Y.; Liu, K.; Liu, J.; He, H. Effects of SO2 on standard and fast SCR over CeWO: A quantitative study of the reaction pathway and active sites. *Appl. Catal. B* **2022**, *301*, 120784.
(51) Kwon, D. W.; Nam, K. B.; Hong, S. C. The role of ceria on the activity and SO_2 resistance of catalysts for the selective catalytic reduction of NOx by NH_3. *Appl. Catal. B* **2015**, *166−167*, 37−44.
(52) Sheng, Z.; Hu, Y.; Xue, J.; Wang, X.; Liao, W.; et al. SO_2 poisoning and regeneration of Mn-Ce/TiO_2 catalyst for low temperature NO_x reduction with NH_3. *Joural of Rare Earths* **2012**, *30* (7), 676.
(53) Zhang, X.; Liu, S.; Ma, K.; Chen, Y.; Jin, S.; Wang, X.; Wu, X. Study on the Mechanism of SO_2 Poisoning of MnO_x/PG for Lower Temperature SCR by Simple Washing Regeneration. *Catalysts* **2021**, *11*, 1360.
(54) Jiang, B. Q.; Wu, Z. B.; Liu, Y.; Lee, S. C.; Ho, W. K. DRIFT study of the SO_2 effect on low-temperature SCR reaction over Fe-Mn/TiO_2. *J. Phys. Chem. C* **2010**, *114* (11), 4961−4965.
(55) Yu, J.; Guo, F.; Wang, Y.; Zhu, J.; Liu, Y.; Su, F.; Gao, S.; Xu, G. Sulfur poisoning resistant mesoporous Mn-base catalyst for low-temperature SCR of NO with NH_3. *Appl. Catal. B* **2010**, *95* (1−2), 160−168.
(56) Xiong, S.; Liao, Y.; Xiao, X.; Dang, H.; Yang, S. The mechanism of the effect of H_2O on the low temperature selective catalytic reduction of NO with NH_3 over Mn-Fe spinel. *Catalysis Science & Technology* **2015**, *5*, 2132.
(57) Phil, H. H.; Reddy, M. P.; Kumar, P. A.; Ju, L. K.; Hyo, J. S. SO_2 resistant antimony promoted V_2O_5/TiO_2 catalyst for NH_3-SCR of NO_x at low temperatures. *Appl. Catal. B* **2008**, *78* (3−4), 301−308.
(58) Liu, F.; He, H. Selective catalytic reduction of NO with NH_3 over manganese substituted iron titanate catalyst: Reaction mechanism and H_2O/SO_2 inhibition mechanism study. *Catal. Today* **2010**, *153* (3−4), 70−76.
(59) Ma, K.; Guo, K.; Li, L.; Zou, W.; Tang, C.; Dong, L. Cavity size dependent SO_2 resistance for NH_3-SCR of hollow structured CeO_2-TiO_2 catalysts. *Catal. Commun.* **2019**, *128*, 105719.
(60) Irfan, M. F.; Goo, J. H.; Kim, S. D. Co_3O_4 based catalysts for NO oxidation and NO_x reduction in fast SCR process. *Appl. Catal. B* **2008**, *78*, 267.
(61) Carja, G.; Kameshima, Y.; Okada, K.; Madhusoodana, C. D. Mn-Ce/ZSM5 as a new superior catalyst for NO reduction with NH_3. *Appl. Catal. B* **2007**, *73*, 60.
(62) Liu, Z.; Yi, Y.; Zhang, S.; Zhu, T.; Zhu, J.; Wang, J. Selective catalytic reduction of NO_x with NH_3 over Mn-Ce mixed oxide catalyst at low temperatures. *Catal. Today* **2013**, *216*, 76−81.
(63) Chen, J.; Fu, P.; Lv, D.; Chen, Y.; Fan, M.; Wu, J.; Meshram, A.; Mu, B.; Li, X.; Xia, Q. Unusual positive effect of SO_2 on Mn-Ce mixed-oxide catalyst for the SCR reaction of NOx with NH_3. *Chem. Eng. J.* **2021**, *407*, 127071.
(64) Yang, S.; Wang, C.; Li, J.; Yan, N.; Ma, L.; Chang, H. Low temperature selective catalytic reduction of NO with NH_3 over Mn−Fe spinel: Performance, mechanism and kinetic study. *Appl. Catal. B* **2011**, *110*, 71.
(65) Meng, D.; Zhan, W.; Guo, Y.; Guo, Y.; Wang, L.; Lu, G. A Highly Effective Catalyst of Sm-MnO_x for the NH_3-SCR of NOx at Low Temperature: Promotional Role of Sm and Its Catalytic Performance. *ACS Catal.* **2015**, *5* (10), 5973.

https://doi.org/10.1021/acsomega.2c06796
ACS Omega 2023, 8, 7262−7278

(66) Qin, Q.; Chen, K.; Xie, S.; Li, L.; Ou, X.; Wei, X.; Luo, X.; Dong, L.; Li, B. Enhanced SO_2 and H_2O resistance of $MnTiSnO_y$ composite oxide for NH_3-SCR through Sm modification. *Appl. Surf. Sci.* **2022**, *583*, 152478.
(67) Xu, J.; Li, H.; Liu, Y.; Huang, L.; Zhang, J.; Shi, L.; Zhang, D. In situ fabrication of porous $MnCo_xO_y$ nanocubes on ti mesh as high performance monolith de-NO_x catalysts. *RSC Adv.* **2017**, *7*, 36319.
(68) Liu, F.; He, H. Structure−Activity Relationship of Iron Titanate Catalysts in the Selective Catalytic Reduction of NO_x with NH_3. *J. Phys. Chem. C* **2010**, *114*, 16929.
(69) Chang, H.; Chen, X.; Li, J.; Ma, L.; Wang, C.; Liu, C.; Schwank, J. W.; Hao, J. Improvement of Activity and SO_2 Tolerance of Sn-Modified MnO_x−CeO_2 Catalysts for NH_3-SCR at Low Temperatures. *Environ. Sci. Technol.* **2013**, *47* (10), 5294−5301.
(70) Xiong, Y.; Tang, C.; Yao, X.; Zhang, L.; Li, L.; Wang, X.; Deng, Y.; Gao, F.; Dong, L. Effect of metal ions doping (M = Ti^{4+}, Sn^{4+}) on the catalytic performance of MnO_x/CeO_2 catalyst for low temperature selective catalytic reduction of NO with NH_3. *Appl. Catal. A* **2015**, *495*, 206−216.
(71) Jiang, B.; Deng, B.; Zhang, Z.; Wu, Z.; Tang, X.; Yao, S.; Lu, H. Effect of Zr Addition on the Low-Temperature SCR Activity and SO_2 Tolerance of Fe−Mn/Ti Catalysts. *J. Phys. Chem. C* **2014**, *118*, 14866−14875.
(72) Obrist, D.; Zielinska, B.; Perlinger, J. A. Accumulation of polycyclic aromatic hydrocarbons (PAHs) and oxygenated PAHs (OPAHs) in organic and mineral soil horizons from four U.S. remote forests. *Chemosphere* **2015**, *134*, 98.
(73) Wu, Z.; Jiang, B.; Liu, Y.; Zhao, W.; Guan, B. Experimental study on a low-temperature SCR catalyst based on MnO_x/TiO_2 prepared by sol-gel method. *JOURNAL OF HAZARDOUS MATERIALS* **2007**, *145* (3), 488−494.
(74) Ettireddy, P. R.; Ettireddy, N.; Mamedov, S.; Boolchand, P.; Smirniotis, P. G. Surface characterization studies of TiO_2 supported manganese oxide catalysts for low temperature SCR of NO with NH_3. *Appl. Catal. B* **2007**, *76*, 123.
(75) Smirniotis, P. G.; Pena, D. A.; Uphade, B. S. Low-Temperature Selective Catalytic Reduction (SCR) of NO with NH_3 by Using Mn, Cr, and Cu Oxides Supported on Hombikat TiO_2. *Angew. Chem., Int. Ed.* **2001**, *40*, 2479.
(76) Shen, B.; Wang, Y.; Wang, F.; Liu, T. The effect of Ce−Zr on NH_3-SCR activity over $MnO_{x(0.6)}/Ce_{0.5}Zr_{0.5}O_2$ at low temperature. *Chemical Engineering Journal* **2014**, *236*, 171−180.
(77) Kylhammar, L.; Carlsson, P.-A.; Ingelsten, H. H.; Grönbeck, H.; Skoglundh, M. Regenerable ceria-based SO_x traps for sulfur removal in lean exhausts. *Appl. Catal. B* **2008**, *84*, 268.
(78) Pourkhalil, M.; Moghaddam, A. Z.; Rashidi, A.; Towfighi, J.; Mortazavi, Y. Preparation of highly active manganese oxides supported on functionalized MWNTs for low temperature NO_x reduction with NH_3. *Appl. Surf. Sci.* **2013**, *279*, 250−259.
(79) Deng, H.; Yi, H.; Tang, X.; Liu, H.; Zhou, X. Interactive Effect for Simultaneous Removal of SO_2, NO, and CO_2 in Flue Gas on Ion Exchanged Zeolites. *Ind. Eng. Chem. Res.* **2013**, *52* (20), 6778−6784.
(80) Yi, H.; Deng, H.; Tang, X.; Yu, Q.; Zhou, X.; Liu, H. Adsorption equilibrium and kinetics for SO_2, NO, CO_2 on zeolites FAU and LTA. *Journal of Hazardous Materials* **2012**, *203-204*, 111−117.
(81) Jin, R.; Liu, Y.; Wang, Y.; Cen, W.; Wu, Z.; Wang, H.; Weng, X. The role of cerium in the improved SO_2 tolerance for NO reduction with NH_3 over Mn-Ce/TiO_2 catalyst at low temperature. *Appl. Catal. B* **2014**, *148−149*, 582−588.
(82) Liu, G.; Zhang, W.; He, P.; Shen, D.; Wu, C.; Gong, C. Effect of Transition Metal Additives on the Catalytic Performance of Cu−Mn/SAPO-34 for Selective Catalytic Reduction of NO with NH_3 at Low Temperature. *Catalysts* **2019**, *9* (8), 685.
(83) You, X.; Sheng, Z.; Yu, D.; Yang, L.; Xiao, X.; Wang, S. Influence of Mn/Ce ratio on the physicochemical properties and catalytic performance of graphene supported MnO_x-CeO_2 oxides for NH_3-SCR at low temperature. *Appl. Surf. Sci.* **2017**, *423*, 845−854.
(84) Wu, Z.; Jin, R.; Wang, H.; Liu, Y. Effect of ceria doping on SO_2 resistance of Mn/TiO_2 for selective catalytic reduction of NO with NH_3 at low temperature. *Catal. Commun.* **2009**, *10* (6), 935−939.
(85) Wang, X.; Wu, S.; Zou, W.; Yu, S.; Gui, K.; Dong, L. Fe-Mn/Al_2O_3 catalysts for low temperature selective catalytic reduction of NO with NH_3. *Chinese Journal of Catalysis* **2016**, *37*, 1314.
(86) Shen, B.-X.; Liu, T. Deactivation of MnO_x-CeO_x/ACF Catalysts for Low-Temperature NH_3-SCR in the Presence of SO_2. *Acta Physico-Chimica Sinica* **2010**, *26* (11), 3009−3016.
(87) Sun, P.; Guo, R.-t.; Liu, S.-m.; Wang, S.-x.; Pan, W.-g.; Li, M.-y. The enhanced SCR performance and SO_2 resistance of Mn/TiO_2 catalyst by the modification with Nb: A mechanistic study. *Appl. Surf. Sci.* **2017**, *531*, 129.
(88) Li, W.; Zhang, C.; Li, X.; Tan, P.; Zhou, A.; Fang, Q.; Chen, G. Ho-modified Mn-Ce/TiO_2 for low-temperature SCR of NO_x with NH_3:Evaluation and characterization. *Chinese Journal of Catalysis* **2018**, *39* (10), 1653−1663.
(89) Chen, L.; Ren, S.; Liu, W.; Yang, J.; Chen, Z.; Wang, M.; Liu, Q. Low-temperature NH_3-SCR activity of M (M = Zr, Ni and Co) doped MnO_x supported biochar catalysts. *J. Environ. Chem. Eng.* **2021**, *9*, 106504.
(90) Wu, B.; Liu, X. Q.; Xiao, P.; Wang, S. G. TiO_2-Supported Binary Metal Oxide Catalysts for Low-temperature Selective Catalytic Reduction of NO_x with NH_3. *Chemical Journal of Chinese Universities* **2008**, *24* (5), 615.
(91) Song, C.; Zhang, L.; Li, Z.; Lu, Y.; Li, K. Co-Exchange of Mn: A Simple Method to Improve Both the Hydrothermal Stability and Activity of Cu−SSZ-13 NH_3−SCR Catalysts. *Catalysts* **2019**, *9* (5), 455.
(92) Zhang, S.; Zhang, C.; Wang, Q.; Ahn, W. S. Co- and Mn-Coimpregnated ZSM-5 Prepared from Recycled Industrial Solid Wastes for Low-Temperature NH_3-SCR. *Ind. Eng. Chem. Res.* **2019**, *58*, 22857.
(93) Gao, R.; Zhang, D.; Liu, X.; Shi, L.; Maitarad, P.; Li, H.; Zhang, J.; Cao, W. Enhanced catalytic performance of V_2O_5−$WO_3/Fe_2O_3/TiO_2$ microspheres for selective catalytic reduction of NO by NH_3. *Catalysis Science & Technology* **2013**, *3* (1), 191−199.
(94) Liu, Y.; Xu, J.; Li, H.; Cai, S.; Hu, H.; Fang, C.; Shi, L.; Zhang, D. Rational design and in situ fabrication of MnO_2@$NiCo_2O_4$ nanowire arrays on Ni foam as high-performance monolith de-NO_x catalysts. *J.mater.chem.a* **2015**, *3* (21), 11543−11553.
(95) Cheng, M.; Jiang, B.; Yao, S.; Han, J.; Zhao, S.; Tang, X.; Zhang, J.; Wang, T. The Mechanism of NH_3-SCR Reaction for NO_x Removal from Diesel Engine Exhaust and Hydrothermal Stability of Cu-Mn/Zeolite Catalysts. *J. Phys. Chem. C* **2018**, *122*, 455.
(96) Li, C.; Tang, X.; Yi, H.; Wang, L.; Cui, X.; Chu, C.; Li, J.; Zhang, R.; Yu, Q. Rational design of template-free MnO_x-CeO_2 hollow nanotube as de-NO_x catalyst at low temperature. *Appl. Surf. Sci.* **2018**, *428*, 924−932.
(97) Gao, F.; Tang, X.; Sani, Z.; Yi, H.; Zhao, S.; Yu, Q.; Zhou, Y.; Shi, Y.; Ni, S. Spinel-structured Mn−Ni nanosheets for NH_3-SCR of NO with good H_2O and SO_2 resistance at low temperature. *Catalysis Science & Technology* **2020**, *10*, 7486.
(98) Zhang, L.; Shi, L.; Huang, L.; Zhang, J.; Gao, R.; Zhang, D. Rational Design of High-Performance DeNO_x Catalysts Based on $Mn_xCo_{3-x}O_4$ Nanocages Derived from Metal−Organic Frameworks. *ACS Catal.* **2014**, *4* (6), 1753−1763.
(99) Soh, B. W.; Nam, I. S. Effect of Support Morphology on the Sulfur Tolerance of V_2O_5/Al_2O_3 Catalyst for the Reduction of NO by NH_3. *Ind. Eng. Chem. Res.* **2003**, *42*, 2975.
(100) Guo, K.; Fan, G.; Gu, D.; Yu, S.; Ma, K.; Liu, A.; Tan, W.; Wang, J.; Du, X.; Zou, W.; Tang, C.; Dong, L. Pore Size Expansion Accelerates Ammonium Bisulfate Decomposition for Improved Sulfur Resistance in Low-Temperature NH_3-SCR. *ACS Appl. Mater. Interfaces* **2019**, *11* (5), 4900−4907.
(101) Jiang, B.; Liu, Y.; Wu, Z. Low-temperature selective catalytic reduction of NO on MnO_x /TiO_2 prepared by different methods. *Journal of Hazardous Materials* **2009**, *162* (2−3), 1249−1254.

https://doi.org/10.1021/acsomega.2c06796
ACS Omega 2023, 8, 7262−7278

(102) Yao, X.; Kong, T.; Chen, L.; Ding, S.; Yang, F.; Dong, L. Enhanced low-temperature NH_3-SCR performance of MnO_x/CeO_2 catalysts by optimal solvent effect. *Appl. Surf. Sci.* **2017**, *420*, 407−415.
(103) Zhang, D.; Zhang, L.; Shi, L.; Fang, C.; Li, H.; Gao, R.; Huang, L.; Zhang, J. In situ supported MnO_x-CeO_x on carbon nanotubes for the low-temperature selective catalytic reduction of NO with NH_3. *Nanoscale* **2013**, *5*, 1127−1136.
(104) Sheng, Z.; Hu, Y.; Xue, J.; Wang, X.; Liao, W. A novel co-precipitation method for preparation of Mn-Ce/TiO_2 composites for NO_x reduction with NH_3 at low temperature. *Environmental Technology* **2012**, *33* (19−21), 2421−2428.
(105) Shi, Y.; Chen, S.; Sun, H.; Shu, Y.; Quan, X. Low-temperature selective catalytic reduction of NO_x with NH_3 over hierarchically macro-mesoporous Mn/TiO_2. *Catal. Commun.* **2013**, *42*, 10−13.
(106) Zou, C.; Wu, X.; Meng, H.; Du, Y.; Li, Z. The SO_2 Resistance Improvement of Mn-Fe/ZSM-5 for NH_3-SCR at Low Temperature by Optimizing Synthetic Method. *Chemistryselect* **2018**, *3*, 13042.
(107) Huang, L.; Hu, X.; Yuan, S.; Li, H.; Yan, T.; Shi, L.; Zhang, D. Photocatalytic preparation of nanostructured MnO_2-(Co_3O_4)/TiO_2 hybrids: The formation mechanism and catalytic application in SCR de$NO_{(x)}$ reaction. *Appl. Catal. B* **2017**, *203*, 778−788.

https://doi.org/10.1021/acsomega.2c06796
ACS Omega 2023, 8, 7262−7278